Dissertations and Theses (Open Access)

MD Anderson UTHealth Houston Graduate School

8-2011

Uptake And Metabolism Of 5'-Amp In The Erythrocyte Play Key Roles In The 5'-Amp Induced Model Of Deep Hypometabolism

Isadora Daniels

Recommended Citation

Daniels, Isadora, "Uptake And Metabolism Of 5'-Amp In The Erythrocyte Play Key Roles In The 5'-Amp Induced Model Of Deep Hypometabolism" (2011). *Dissertations and Theses (Open Access)*. 176.
https://digitalcommons.library.tmc.edu/utgsbs_dissertations/176

UPTAKE AND METABOLISM OF 5'-AMP IN THE ERYTHROCYTE PLAY KEY

ROLES IN THE 5'-AMP INDUCED MODEL OF DEEP HYPOMETABOLISM

by

Isadora Susan Daniels, B.A.

APPROVED:

_____

Cheng Chi Lee, Ph.D.
Supervisory Professor

_____

Diane Bick, Ph.D.

_____

Michael R. Blackburn, Ph.D.

_____

Rodney Kellems, Ph.D.

_____

Ann-Bin Shyu, Ph.D.

APPROVED:

_____

Dean, The University of Texas
Graduate School of Biomedical
Sciences

UPTAKE AND METABOLISM OF 5'-AMP IN THE ERYTHROCYTE PLAY KEY

ROLES IN THE 5'-AMP INDUCED MODEL OF DEEP HYPOMETABOLISM

A

DISSERTATION

Presented to the Faculty of

The University of Texas

Health Science Center at Houston

and

The University of Texas

M.D. Anderson Cancer Center

Graduate School of Biomedical Sciences

in Partial Fulfillment

of the Requirements

for the Degree of

DOCTOR OF PHILOSOPHY

by

Isadora Susan Daniels, B.A.

Houston, Texas

August, 2011

UPTAKE AND METABOLISM OF 5'-AMP IN THE ERYTHROCYTE PLAY KEY ROLES IN THE 5'-AMP INDUCED MODEL OF DEEP HYPOMETABOLISM

Publication No. _____

Isadora Susan Daniels, B.A.

Supervisory Professor: Cheng Chi Lee, Ph.D.

Mechanisms that initiate and control the natural hypometabolic states of mammals are poorly understood. The laboratory developed a model of deep hypometabolism (DH) initiated by uptake of 5'-adenosine monophosphate (5'-AMP) into erythrocytes. Mice enter DH when given a high dose of 5'-AMP and the body cools readily. Influx of 5'-AMP appears to inhibit thermoregulatory control. In a 15°C environment, mice injected with 5'-AMP (0.5 mg/gw) enter a Phase I response in which oxygen consumption (VO_2) drops rapidly to $1/3^{rd}$ of euthermic levels. The Phase I response appears independent of body temperature (T_b). This is followed by gradual body temperature decline that correlates with VO_2 decline, called Phase II response. Within 90 minutes, mouse T_b approaches 15°C, and VO_2 is $1/10^{th}$ of normal. Mice can remain several hours in this state, before gradually and safely recovering. The DH state translates to other mammalian species. Our studies show uptake and metabolism of 5'-AMP in erythrocytes causes biochemical changes that initiate DH. Increased AMP shifts the adenylate equilibrium toward ADP formation, consequently decreasing intracellular ATP. In turn, glycolysis slows, indicated by increased glucose and decreased lactate. 2,3-bisphosphoglycerate levels rise,

allosterically reducing oxygen affinity for hemoglobin, and deoxyhemoglobin rises. Less oxygen transport to tissues likely triggers the DH model.

The major intracellular pathway for AMP catabolism is catalyzed by AMP deaminase (AMPD). Multiple AMPD isozymes are expressed in various tissues, but erythrocytes only have AMPD3. Mice lacking AMPD3 were created to study control of the DH model, specifically in erythrocytes. Telemetric measurements demonstrate lower T_b and difficulty maintaining T_b under moderate metabolic stress. A more dramatic response to lower dose of 5'-AMP suggests AMPD activity in the erythrocyte plays an important role in control of the DH model. Analysis of adenylates in erythrocyte lysate shows 3-fold higher levels of ATP and ADP but similar AMP levels to wild-type.

Taken together, results indicate alterations in energy status of erythrocytes can induce a hypometabolic state. AMPD3 control of AMP catabolism is important in controlling the DH model. Genetically reducing AMP catabolism in erythrocytes causes a phenotype of lower T_b and compromised ability to maintain temperature homeostasis.

Table of Contents

List of Illustrations

List of Tables

List of Abbreviations

(alphabetical)

1,3-BPG, 1,3-bisphosphoglycerate

2,3-BPG, 2,3-bisphosphoglycerate

2-DG, 2-deoxyglucose

5'-AMP, 5'-adenosine monophosphate

5'-CMP, 5'-cytidine monophosphate

5'-GMP, 5'-guanosine monophosphate

ACN, acetonitrile

Ado, adenosine

ADP, adenosine diphosphate

AMPD, adenosine monophosphate deaminase

ATP, adenosine triphosphate

BSA, bovine serum albumin

cAMP, 3',5'-cyclic adenosine monophosphate

cDNA, complementary DNA

CLAMS, Comprehensive Lab Animal Monitoring System

DH, deep hypometabolism

HPLC, high performance liquid chromatography

HPc, hibernation-specific protein complex

Hx, hypoxanthine

i.p., intraperitoneal

i.v., intravenous

IMP, inosine monophosphate

Ino, inosine

RT-PCR, reverse transcription polymerase chain reaction

s.q., subcutaneous

T_a, ambient temperature

T_b, core body temperature

TLC, thin layer chromatography

UCP1, uncoupling protein 1

VO_2, oxygen consumption in ml/kg/hr

Xan, xanthine

Chapter 1
Overview of natural hypometabolism and therapeutic hypothermia

Overview of natural methods of energy conservation

Mammals and birds have high metabolic rates and generate large amounts of heat even while at rest, allowing them to maintain a constant core body temperature (T_b) of about 37°C. They can maintain normal T_b (euthermia) despite losing body heat to a cold environment, by increasing heat production. This trait comes at high energy cost and allows mammals and birds to live in extreme environments including below freezing temperatures (1).

Some mammals and birds can undergo hypometabolic periods that allow energy conservation. Most mammals experience shallow oscillations in metabolic rate by up to 20% during the 24 hour rhythm of rest and activity. There is a corresponding fluctuation in T_b, ranging from 0.5 to 2°C. Birds experience more pronounced oscillations in metabolic rate and T_b (1).

In addition to the 24 hourly rhythm, many mammals and birds can undergo extended periods of hypometabolism and reduced T_b. Some mammals experience a daily temporary decline in metabolic rate and T_b, called daily torpor, often in response to changes in photoperiod, decreased food availability, and colder ambient temperature (T_a) (2). In response to lack of water in warm environments, reptiles and amphibians undergo aestivation, which is a hypometabolic state similar to torpor but without the decrease in T_b (3). Aestivation is rare in mammals, the best described is the fat-tailed dwarf lemur in the tropics (4). Some mammals undergo a seasonal extended period of deep torpor bouts, called hibernation. In

daily torpor, aestivation and hibernation, metabolic rate can be reduced to a fraction of the basal rate (1).

Among the diverse species of mammals, many orders, including carnivora, primates, and rodentia have members that either hibernate or undergo daily torpor. A large range of sizes of mammals can enter such hypometabolic states, from shrews to bears. Hibernation experts suggest that this means all mammals share a widespread ability to enter a hypometabolic state (1).

During hibernation an animal's metabolic rate and T_b decreases in torpor bouts that can last for several weeks, with periodic arousals to euthermia lasting about one day. Small hibernators such as bats, marmots and ground squirrels, can undergo a dramatic decrease in T_b, reaching temperatures close to or below freezing. The metabolic rate of these small hibernators decreases to approximately 2-5% of basal metabolic rate (5). However, a much larger hibernating mammal such as the bear undergoes a less dramatic change in T_b and metabolic rate. For this reason, investigators in the hibernation field debated whether bears are true hibernators. Recently, continuous telemetry and metabolic rate monitoring performed in black bears led to the conclusion that they do hibernate. Bear T_b declines from 37°C to a low of 30°C, with an average temperature of 33°C. Metabolic rate of bears decreases to between 53 – 65% of normal rate (5). Even tropical primates can hibernate. The fat-tailed dwarf lemur of Madagascar lives on fruits and arthropods in the dry deciduous forest of Kirindy. During the dry season the animals hibernate or aestivate in tree holes in response to food and water

shortage. The T_b of these animals can fluctuate widely, depending on the T_a, and they remain hypometabolic even when the T_a is above 30°C (4).

The mechanisms that initiate hypometabolic states such as torpor, aestivation and hibernation are poorly understood. Environmental conditions that can trigger these states are short photoperiod, cold T_a (in torpor), warm T_a (in aestivation), and less food and water availability. Animals such as deer mice and hamsters enter torpor in response to short photoperiod, even with free access to food and water. However, food shortage can induce torpor in these animals during any season (6). For decades investigators have tried to determine the molecular and biochemical conditions that cause animals to enter such hypometabolic states.

Investigators have identified a complex of four proteins called hibernation-specific protein complex (HPc) that is a candidate hormone for control of hibernation. It is produced in the liver, enters the bloodstream, and its expression and transport into the brain are regulated by endogenous circannual rhythms (7). In chipmunks, levels of HPc begin to decline in blood, and begin a simultaneous increase in cerebrospinal fluid, prior to onset of hibernation. Levels remain low in blood and peak in cerebrospinal fluid during the hibernation phase. At the end of hibernation, HPc levels rise in blood and decline in cerebrospinal fluid. The circannual changes in HPc levels are independent of changes in body temperature, which raised questions to its correlation with the animal's metabolic state (8).

Interestingly, in European hamsters it was found that the circadian clock is stalled during deep torpor. The mRNA levels of three of the genes involved in the

4

transcriptional feedback loop that drives the circadian clock were compared in euthermic and hibernating hamsters. In contrast to the normal oscillation of mRNA levels of Per1, Per2, and Bmal1 in euthermic animals, the transcripts in the hibernating animals remained at steady levels, showing that the circadian clock was no longer oscillating (9). However, the circadian clock appears to regulate the timing of torpor behavior. It was shown that ablation of the hypothalamic suprachiasmatic nucleus, the structure of the brain that is the pacemaker for the circadian clock, changes timing of hibernation in ground squirrels (10).

Energy utilization in natural hypometabolic states

Energy sources were studied in Djungarian hamsters in torpor. It was found that during the beginning of a torpor bout the animals primarily used carbohydrates for energy, but that as the torpor bout progressed there is a progression towards lipid metabolism as their primary energy source. (11).

Control of body temperature by the hypothalamus

The preoptic area of the hypothalamus is thought to play a central role in regulating T_b. When T_b decreases, the preoptic area sends a signal to the vasomotor center in the medulla to trigger an autonomic response that decreases the diameter of peripheral blood vessels. In turn, this reduces blood flow to the skin, which reduces the rate of heat loss to the environment (12). However, if the vasomotor center is inhibited, peripheral vasodilation occurs, and the increased blood flow to the skin causes heat loss to the environment. When the blood flow increases, the sweat glands are stimulated, and this increases evaporative heat

loss. In addition, respiration rate is increased, which also causes heat loss through evaporation (12). All these changes that control the T_b are thought to be triggered by the preoptic area of the hypothalamus.

Cold and warm-sensitive neurons exist in the hypothalamus. Mice over-expressing the uncoupling protein 2 in hypocretin neurons were found to have elevated temperature in the hypothalamus. These mice displayed a phenotype of lower T_b by $0.3 – 0.5°C$ compared to wild-type littermates (13).

Thermogenesis by uncoupling oxidative phosphorylation

Uncoupling proteins act to uncouple the oxidation (electron transport chain) from the phosphorylation (generating ATP from ADP) in oxidative phosphorylation (14). The classical uncoupling protein, UCP1, is located in the inner membrane of mitochondria in brown adipose tissue. It uses oxygen to combust substrate, and releases heat without producing ATP. This allows non-shivering thermogenesis (14). Adult humans and most large adult mammals do not have much brown adipose tissue, but it is found in many adult small mammals and in newborn mammals (14, 15). Uncoupling of oxidative phosphorylation is known to generate heat to maintain T_b in many hibernating mammals, mammals adapted to cold T_a, and in newborn mammals (16). Other uncoupling proteins, UCP2 and UCP3 have been identified in other tissues, but there is ongoing debate about their roles in thermogenesis (15).

Artificial induction of hypometabolism

While the initiation mechanism of hypometabolism seen in hibernation and torpor is still unknown, glucose metabolism appears to play a role. Siberian hamsters can be induced into torpor by injection of 2-deoxyglucose (2-DG), a metabolic inhibitor (17). 2-DG is a non-metabolizable analog of glucose that inhibits the first enzyme in the glycolytic pathway, hexokinase. The length of the torpor bouts can be modulated with short photoperiods. These observations implicate the cellular production of ATP to be important for torpor. However, injection of a different metabolic inhibitor, β-mercaptoacetate, which inhibits fatty acid oxidation in mitochondria, does not induce torpor in these animals (17). These observations suggest that the glycolytic pathway appears to play a key role in the induction of torpor. In contrast, fatty acid oxidation does not appear to play a role in the induction.

Another substance used to induce a torpor state in animals is 3-iodothyronamine, a naturally occurring metabolite of T_4, which is the most active form of thyroid hormone. When rodents were given a large dose of 3-iodothyronamine, they entered a hypometabolic state and had lowered heart rate. Research is ongoing to determine the mechanism, which has been shown to be active without entry into the brain. G-protein coupled receptor signaling is believed to be involved (18, 19).

Microinjection of adenosine into the anteroventral preoptic region of the brain was shown to induce hypothermia and simultaneous hypoxia-induced

hyperventilation in rats. This mechanism is believed to act through the A_1 adenosine receptor, because injection of an A_1 receptor – specific antagonist attenuated these effects (20).

A model of "suspended animation" was developed in non-hibernating mammals that is induced by inhalation of H_2S gas. In the H_2S model, animals enter a hypometabolic state and lose ability to thermoregulate (21, 22). The H_2S gas induction of hypometabolism is thought to be through its inhibition of cytochrome c oxidase activity. However, H_2S gas is known to be rapidly taken up by the red blood cells and has been shown to dissociate oxygen from hemoglobin in the reaction $HbO_2 + 2H_2S = Hb + 2H_2O + 2S$ (23).

Another method investigators have used to induce hypometabolism and dramatically decrease T_b in non-hibernating mammals is exsanguination. In this method, replacement of blood with a saline solution can successfully and reversibly reduce T_b of dogs to near freezing (24).

Although mechanisms of hibernation and torpor in the wild are not fully understood, protective benefits of lowered body temperature and metabolic rate are observed. For example, animals in hibernation do not suffer the harmful effects of ischemia despite dramatic decreases in blood flow to tissues (25).

Therapeutic Hypothermia in the Clinic

Clinicians employ these protective benefits by artificially reducing body temperature and metabolic rate in medical trauma cases. Therapeutic hypothermia attenuates further injury in patients who have suffered stroke or myocardial

8

infarction. It is also used during surgeries such as transplant, cardiac bypass, and aortic repair to prevent ischemia-reperfusion injury, a common complication following major surgery (26).

Although more doctors have begun using therapeutic hypothermia in the past decade, the methods are still considered risky because the patient's body naturally fights the decrease in body temperature, requiring administration of paralytic and sedative drugs. The drug effects make it difficult to properly assess and treat the patient (27). This challenge has prompted researchers to look for safer methods of inducing hypothermia.

The goal of this dissertation is to describe my research on our laboratory's model of 5'-AMP – induced deep hypometabolism. It will describe investigations to determine the role of 5'-AMP in the model, the site of initiation, and an aspect of metabolic control of the model. This body of work contributes to the understanding of the mechanisms of the model, which has possible potential for therapeutic use in humans.

Chapter 2

Experimental Procedures

Creation of AMPD3 deficient mice

ES cells containing the vector to make the AMPD3 deficient mice were purchased from Knockout Mouse Project (KOMP), University of California, Davis, CA. The vector was designed using the strategy for "knockout-first" alleles described by the Stewart lab (28). The vector used the "knockout-first" technology to insert the cassette into intron 1 before the essential exon (exon 2) of AMPD3 locus to create a missense mutation that would result in a non-functional mRNA transcript (Figure 1). The ES cells were originally produced by Lexicon (now Lexicon Pharmaceuticals, Inc.), The Woodlands, TX, and then sold to KOMP. The ES cells (C57Bl/6 background) were sent to the Transgenic and Stem Cell Service Unit of the Brown Institute of Molecular Medicine, Houston, TX, for microinjection and generation of chimeras. Eight male chimeras (C57Bl/6 wild-type, Balbc AMPD3 knockout) were generated, and all were mated with C57Bl/6 wild-type females purchased from Harlan Laboratories, Houston, TX. Of the 8 chimeras, 2 were able to produce germline transmission to create AMPD3 $^{+/-}$ mice, which were then mated to produce the AMPD3 $^{+/+}$, $^{+/-}$ and $^{-/-}$ mice used in experiments.

Figure 1: The targeting vector design for AMPD3 knockout

ES Cell Clone (C57Bl/6 background)
Targeting vector – conditional (frameshift)
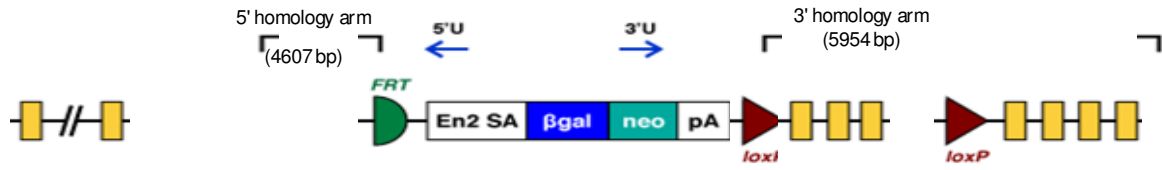
Knock-in vector into exon 2
3' homology arm is in exon 3 and exon 4

Metabolic Chamber description and use

For metabolic chamber experiments, mice were housed in a climate-controlled metabolic chamber designed for mouse studies, the Comprehensive Lab Animal Monitoring System (CLAMS), Columbus Instruments, Columbus, OH. It has 16 cages inside a precisely controlled temperature unit (temperature range 2 - 50°C, +/- 1°C). Each animal is housed individually in an airtight cage, and O_2 and CO_2 going in and out of the cage is measured by high speed gas sensors on an Open Circuit Oxymax Calorimeter, (Columbus Instruments, Columbus, OH). The airflow into and out of the cage is calibrated against a known gas mixture before each experiment. To avoid contamination of the sampled air, the sample flows through Drierite to capture moisture, and ammonia filters capture urea. Samples are taken every minute, cage by cage, with one extra minute for calibration, so if all 16 cages are used, then air in each cage is sampled every 17 minutes. Receivers on the sides of each cage can collect telemetry data, which is measured at the same frequency as the gas sensing. In some of the experiments, animals were implanted with telemetry chips (G2 E-mitter, Mini-Mitter Respironics, Bend, OR). The cages allow free access to food and water. Food consumption can be measured by crushing the mouse chow pellets. The food hopper is on a scale, and as food is removed, the negative balance is recorded. Length and frequency of feeding bouts are also recorded.

Surgical Implantation of Telemetry Chips into Mice

Telemetry chips are sterilized via ethylene oxide gas. Animals are anesthetized via isoflurane gas mask to surgical plane of anesthesia. One dose of antibiotic (Baytril, 5 mg/kg, *s.q.*) is injected at the incision site. One dose of analgesia (Buprenorphine, 0.1 mg/kg, *s.q.*) is injected. The ventral surface of the abdomen is clipped free of hair, and the animal is secured to a heated surgical surface with adhesive tape. The shaved area is disinfected with Betadine. One dose of local analgesic (0.25% Marcaine, < 1 ml/kg) is injected at the incision site. A midline abdominal skin incision of no more than 2 cm is made 1 cm below the diaphragm. Then the abdomen is opened by making a 2 cm incision along the *linea alba* of fascia where the abdominal muscles join the midline. The intestines and colon are gently reflected and the e-mitter is positioned in the abdominal cavity along the saggital plane, placed in front of the caudal arteries and veins but dorsal to the digestive organs. Non-absorbable nylon suture is passed through the silastic tubing in the outer wall of the e-mitter capsule. The capsule is sutured to the body wall to reduce migration of the e-mitter inside the body, and provide a more accurate temperature reading. Organs are replaced, intestines and colon are examined for kinks, and then the abdominal opening is closed with 5-0 Vicryl absorbable suture material using a continuous interlocking running stitch. Then the skin is closed with nylon suture material using interrupted mattress stitches. Then the animal is removed from anesthesia, and given pain relief as needed and monitored for the recovery period. Animals are not used in experiments until two weeks after the surgery and they show signs of full recovery.

AMP Deaminase Activity Assay

This protocol was adapted from a protocol of Dr. Richard Sabina, University of Wisconsin Medical School (e-mail correspondence). AMPD activity is quantified by measuring formation of IMP when protein sample is added to a reaction mixture with saturated amount of substrate (AMP). 20 ug soluble protein is placed in a 1.5 ml tube and the following reaction mixture is added: 25 mM imidazole, pH 7.0, containing 0.2 mg/ml bovine serum albumin (BSA), 150 mM potassium chloride. The mixture is prewarmed in a 37°C water bath and then 20 mM 5'-AMP is added to initiate the assay. Total volume of the reaction mixture is 100 ul. A 50 ul aliquot is removed at 60 minutes, frozen at -80°C, and stored at -20°C. Samples are analyzed by high performance liquid chromatography (HPLC) (Alliance 2695 Separations Module with 2998 Photodiode Array Detector, Waters, Millipore Corp.) using a 5 um C18 reversed phase column (Custom LC, Inc., Houston, TX) and running a gradient of mobile phase 20 mM ammonium phosphate, pH 5.1 with methanol added into the gradient. The gradient is designed as 0-4 minutes 0% methanol, 4-6 minutes 0-8% methanol, 6-8 minutes 8-20% methanol, 8-18 minutes 20% methanol.

Analysis of adenine nucleotides in erythrocyte lysate

Erythrocytes are isolated from whole blood by removing serum and washing 3 times in ice-cold phosphate-buffered saline. Cells are lysed by freeze/thaw and then extracts are made by adding 3 volumes of ice-cold 70% methanol overnight. The supernatant is removed after centrifugation at 12,000 x g at 4°C for 10 minutes. Supernatant is evaporated to dryness and then resuspended in 200 ul mobile phase. The pellet is used to determine protein concentration. Nucleotides in the

extracts are separated by HPLC (Alliance 2695 Separations Module with 2998 Photodiode Array Detector, Waters, Millipore Corp.) using a 5 um C18 reversed phase column (Sunfire, Waters, Millipore Corp.) and running a gradient with mobile phase of 150 mM KH2PO4 and 150 mM KCl, pH 6.0, with superimposed 15% acetonitrile (ACN). The gradient is programmed as 0-20 sec 0% ACN, 20 s – 21 min 0-1.35% ACN, 24 min – 28 min 1.35-15% ACN, 29 min – 35 min 0% ACN. Nucleotides are quantified against standard curves of purchased standards (Sigma-Aldrich, St. Louis, MO).

Chapter 3

Introduction to the 5'-AMP - Induced Model of Deep Hypometabolism

Introduction

The 5'-AMP – induced deep hypometabolism model was a fortuitous discovery in the laboratory, which primarily focuses on circadian rhythm research. A microarray comparing gene expression in liver samples of wild-type mice kept in 12h:12h light/dark cycle or constant darkness found procolipase to be highly expressed during constant darkness (29). Procolipase is a coenzyme for pancreatic triglyceride lipase, and pancreatic lipase related proteins 1 and 2. These proteins catabolize dietary fats into fatty acids and are only expressed in pancreas and gastrointestinal tract, not in liver (30-32). Northern blot analysis of liver mRNA found strong circadian pattern to the procolipase expression in wild-type mice during constant darkness, but not during light-dark cycle. Wild-type mouse tissues expressed procolipase only in stomach and pancreas in normal light/dark cycle, but constant darkness caused expression in many other tissues (29).

Through a series of several experiments tracking the procolipase expression, the observations suggested that procolipase expression is regulated by unknown circulatory factor(s) that control expression during either light/dark cycle or constant darkness. One of the approaches to identify the putative factor included high performance liquid chromatography (HPLC) analysis of blood extracts from mice at various time points in either light/dark cycle or constant darkness. From these studies, it was observed that one of the four reproducible peaks in all the samples had a strong circadian pattern in both the light/dark cycle and in constant darkness. In addition, it was observed that the peak area in samples from constant darkness was elevated compared to light/dark cycle, a feature consistent with the putative

factor. The peak had a maximum absorbance at 260 nm, which suggested it may be a nucleotide. The peak was confirmed to be 5'-AMP (29).

Synthetic 5'-AMP was injected into mice kept in light/dark cycle to test whether it could induce expression of procolipase. Northern blot and RT-PCR analysis demonstrated induced expression of procolipase in all peripheral tissues sampled except for brain. Incidentally, the injection of 5'-AMP was found to induce a transient state of torpor in mice and was observed to decrease core body temperature (T_b) from 37°C to 26°C. (29).

Injection of 5'-AMP induces a deep hypometabolic state which is moderated by ambient temperature

Further studies showed that mice can enter a reversible deep hypometabolic state (DH) that can last several hours after treatment with 5'-AMP. Initial investigations were performed to determine the physical parameters of the DH state. A temperature-controlled Comprehensive Lab Animal Monitoring System (CLAMS) metabolic chamber was used in our studies to measure the physiological effects of the 5'-AMP injection on mice. Mice are housed in individual sealed cages with free access to food and water. Air in the cages is sampled to calculate the oxygen consumption, or VO_2 in units of ml/kg/hr. T_b was measured simultaneously by implanting telemetry chips into the animals (33).

We observed that placing the mice in a cold environment after 5'-AMP injection caused more reduction in T_b compared to T_b of mice in a 23°C environment. The effect of ambient temperature (T_a) on the reduction of T_b of mice

was investigated. The VO_2 and T_b were monitored in mice injected with 0.5 mg/gw 5'-AMP and placed in either a 23°C or 15°C metabolic chamber (Figure 2 a,b). Saline injected mice were used as controls. The saline-injected mice, at both 23°C or 15°C, maintained normal VO_2 levels in the range of 4000 to 6500 ml/kg/h. In addition, they maintained T_b of approximately 37°C regardless of T_a. In contrast, between sampling points (~8 minutes) mice given 5'-AMP displayed a very steep and rapid decrease in VO_2, to below 2000 ml/kg/h, and this occurred in both the 23°C and the 15°C T_a groups. The first decrease in VO_2 is referred to as the Phase I response. However, both T_a groups given 5'-AMP experienced only a small drop in T_b during the Phase I response. The saline injected animals in both groups did not experience a Phase I response, and they maintained euthermic T_b throughout the experiment.

After the Phase I response, the effects of the two T_as diverged in the 5'-AMP injected groups. The decline in VO_2 corresponded with a decrease in T_b. This was classified as the Phase II response, where the decline in T_b corresponds to the further decline in VO_2.

Figure 2: Relationship between VO_2, T_b and T_a following 5'-AMP injection. a and b, simultaneous measurement of T_b and VO_2 of mice given saline or 5'-AMP (0.5 mg/gw, indicated by arrow) in individual metabolic chambers at T_a of 23 and 15 °C. Each mouse used in the study is represented by the same color trace for VO_2 and T_b. Sampling time for both T_b and VO_2 was about 8 min. The colors reflect VO_2 and T_b of independent measurement of different animals given either saline or 5'-AMP. c, respiration rate of mice (*n*=4) with T_b ~16 °C compared with 37 °C. d, heart rate of mice (n=3) with T_b 16 °C compared with 37 °C. *, $p < 0.001$, paired *t* test. Error bars, S.E.M. This research was originally published in The Journal of Biological Chemistry. Daniels IS, Zhang J, O'Brien WG, Tao Z, Miki T, Zhao Z, Blackburn MR, Lee CC. Title. J Biol Chem. 2010; 285:20716-20723. © the American Society for Biochemistry and Molecular Biology.
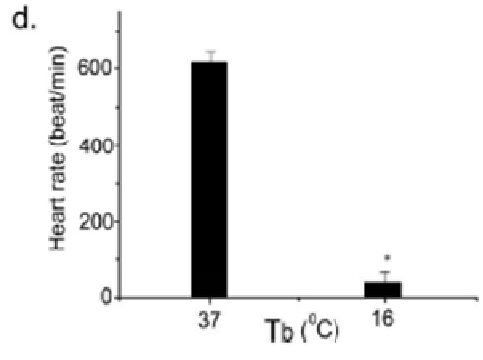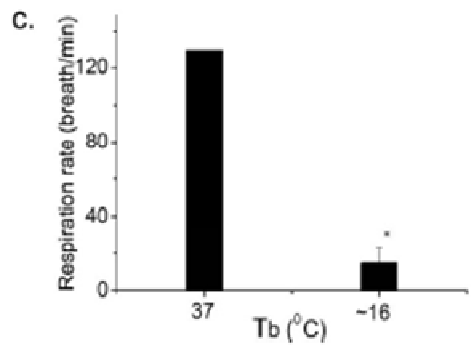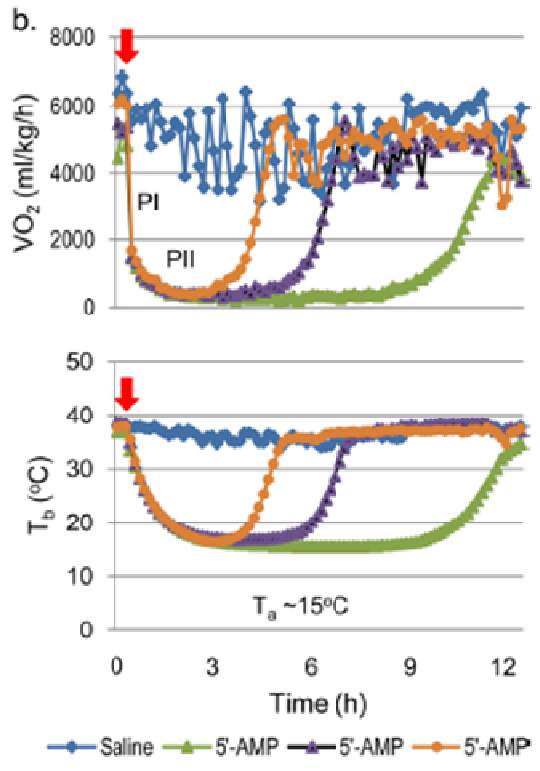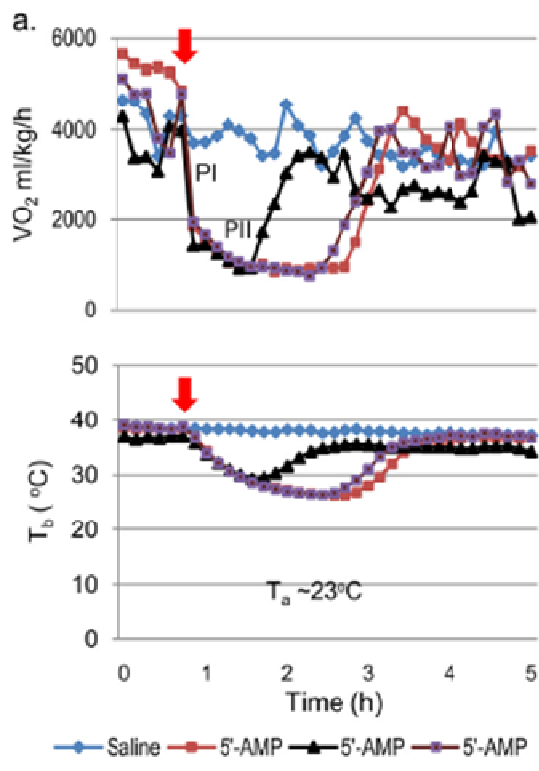
The VO_2 of mice in the 23°C environment reached a lowest point at approximately 1000 ml/kg/h, and their T_bs decreased to approximately 26 – 28°C. In contrast, the mice in the 15°C environment had a more dramatic decrease in VO_2 and T_b, to approximately 300 ml/kg/h and 16°C, respectively. These data show that colder T_a facilitates greater loss of body heat to the environment, allowing the mice in 15°C to reach a lower T_b and attain a much lower VO_2.

The breathing rate and heart rate of mice before and after 5'-AMP injection was also measured. Mice had a normal breathing rate of approximately 120 breaths per minute. After injection of 0.5 mg/gw 5'-AMP, and cooling to a T_b of 16°C, the breathing rate decreased to approximately 10 breaths per minute. There was a similarly dramatic decrease in heart rate, from approximately 600 beats per minute to 50 beats per minute (Figure 2 c,d). These physical measurements indicate that the mice were in an extremely low metabolic state and we regarded them to be in deep hypometabolism (DH).

In summary, the Phase I response is rapid, occurring soon after injection of 5'-AMP, and it is independent of T_b decrease. In contrast, the Phase II VO_2 response is more gradual, and apparently depends on the animal's T_b, which in turn is regulated by T_a. Marked reductions in breathing rate and heart rate accompany the entry into DH.

Observations and description of mice in DH

Distinct physical responses were observed in mice when they enter different degrees of hypometabolism. When the T_b reaches approximately 17°C, they are unable to right themselves when placed on their backs. However, they will respond to stimuli such as touch, but appear to be in a deep stupor. The mice do sometimes scratch, urinate, and roll side to side on their backs when in this state. Based on observations of the animals' behavior, it was determined that mice enter the DH state when T_b reaches 17°C or below. The T_b generally stays one or two degrees above the T_a during the DH state. In our studies, the mice are maintained in the DH state at T_a of 15°C and a T_b of about 16°C. When T_b falls below 14°C, it can be fatal within a few hours.

We observed that mice kept in a 15°C T_a will arouse spontaneously from the DH state. VO_2 and T_b will both rise slowly at first. However, when the T_b reaches approximately 22°C, the mice will start shivering and the VO_2 will rise rapidly. Within two hours their T_b will have returned to euthermia and normal behaviors such as grooming, eating and drinking and social behaviors are apparent. There was no difference in cognitive function of the mice after DH, as evaluated for both long-term and short-term effects by Morris Water maze testing (Figure 3). The animals showed no difference in escape latency. Also, there was no observed difference in lifespan of mice having undergone DH (33). The DH model works equally in male and female mice.

Figure 3: Morris Water Maze escape latency of mice before and after DH. *n* = 20, mice used were 8 weeks old and were trained to escaping from water maze for 6 days before the experiment. The experiment was repeated 3 times and results are presented as +/- S.E.M. No significant difference between DH and before DH.
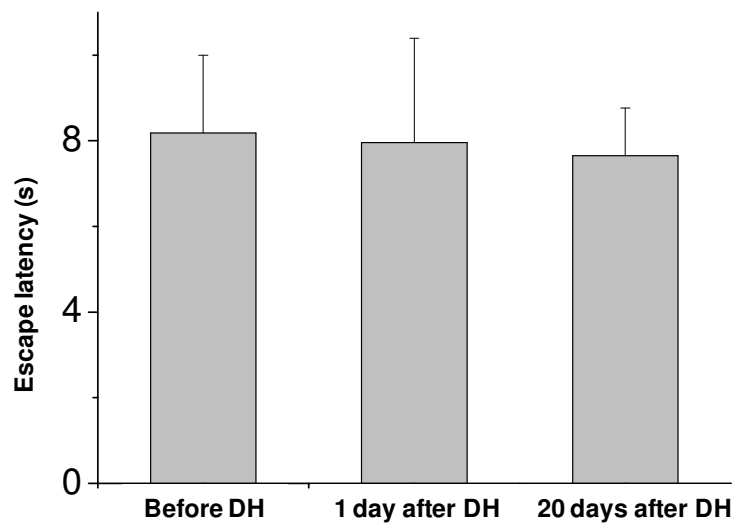
The dose of 5'-AMP induces the DH state but does not control its length

As shown in Figure 2b, the length of time in DH of individual mice is variable, generally lasting from 2-8 hours. The variability of length of time in DH caused us to question whether a larger dose of 5'-AMP could prolong the effect. To investigate the effect of different dosages of 5'-AMP on the length of time in DH, groups of mice with telemetry implants were injected with saline or a dose of 5'-AMP from 0.1 mg/gw to 1 mg/gw and placed in a 15°C CLAMS metabolic chamber (Figure 4 a,b,c,d).

Figure 4: DH as a function of 5'-AMP dosage. a-d, simultaneous measurement of T_b and VO_2 of mice given different dosages of 5'-AMP and maintained at T_a of 15°C. The different colors in the graph reflect VO_2 and T_b of different animals used in the study. This research was originally published in The Journal of Biological Chemistry. Daniels IS, Zhang J, O'Brien WG, Tao Z, Miki T, Zhao Z, Blackburn MR, Lee CC. Title. J Biol Chem. 2010; 285:20716-20723. © the American Society for Biochemistry and Molecular Biology.

a. Saline, $T_a \sim 15°C$ — VO2 (ml/kg/h) and T_b (°C) vs Time (h), Mouse 1, Mouse 2

b. 0.1 mg/g 5'-AMP, $T_a \sim 15°C$ — VO2 (ml/kg/h) and T_b (°C) vs Time (h), Mouse 1, Mouse 2

c. 0.25 mg/g 5'-AMP, $T_a \sim 15°C$ — VO2 (ml/kg/h) and Tb (°C) vs Time (h), Mouse 1, Mouse 2

d. 1.0 mg/g 5'-AMP, $T_a \sim 15°C$ — VO2 (ml/kg/h) and Tb (°C) vs Time (h), Mouse 1, Mouse 2
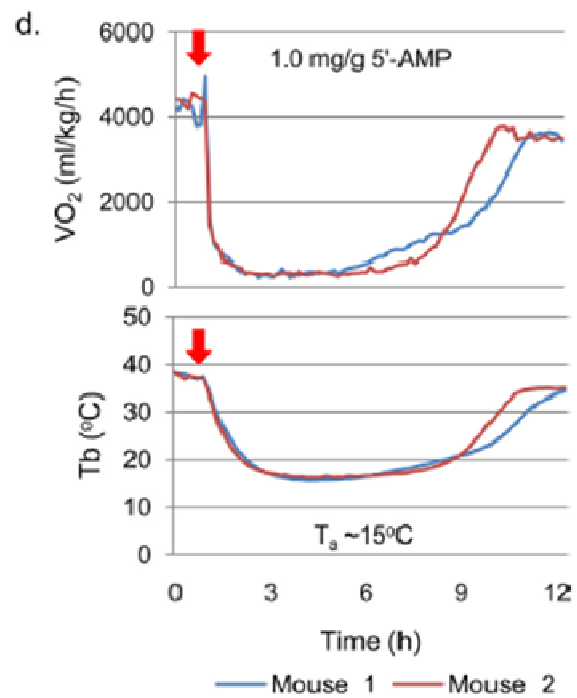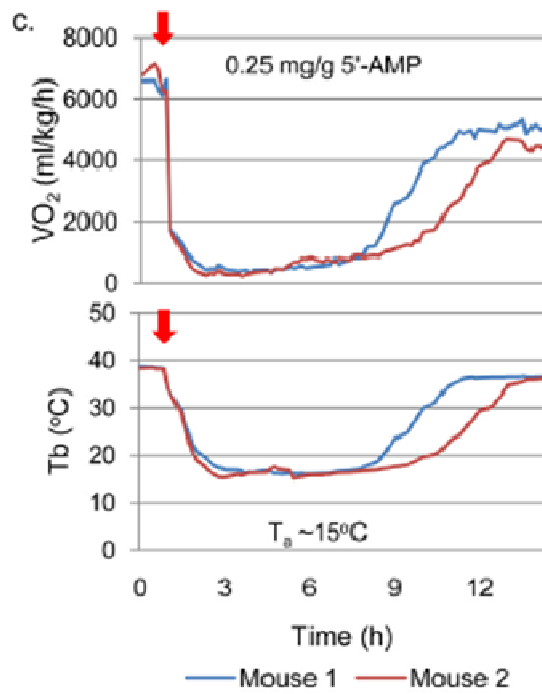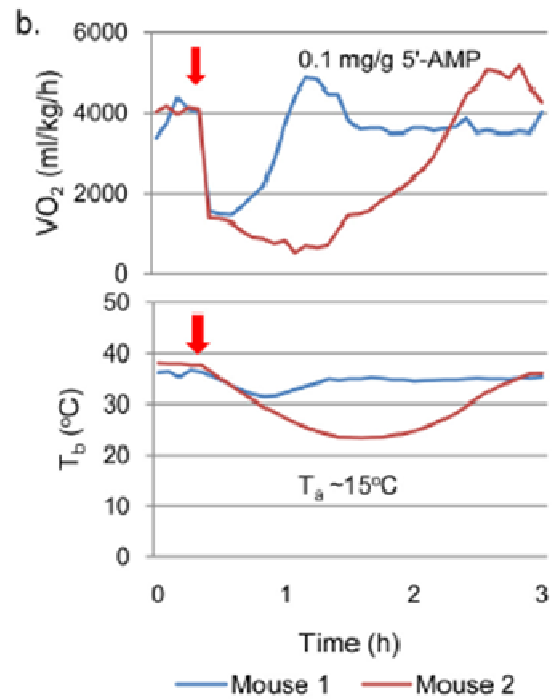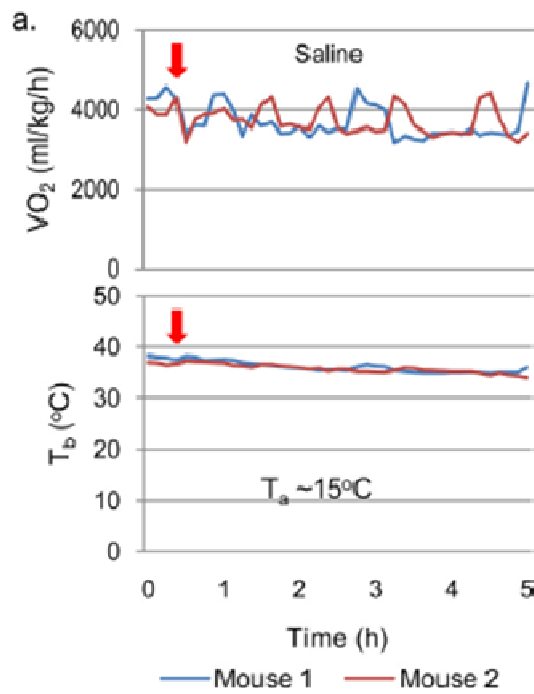
Mice given saline maintained approximately 37 °C T_b under these conditions. The VO_2 had normal fluctuations between 3500 – 4500 ml/kg/h, coinciding with periods of rest and activity. Both mice given 0.1 mg/gw 5'-AMP experienced the Phase I response, and a rapid decrease in VO_2 from 4000 to 1500 ml/kg/h between the sampling points following 5'-AMP administration. One of the animals had a short Phase II response that corresponded with a slight decrease in T_b, but it did not enter DH. The other animal had an aborted Phase II response, and its T_b decreased a few degrees before returning to euthermia. In contrast, mice given 0.25 mg/gw 5'-AMP both experienced the Phase I and Phase II responses, and stayed in DH several hours. Finally, mice given the highest dose, 1.0 mg/gw 5'-AMP, had Phase I and Phase II responses and stayed in DH for similar length as lower doses.

These studies revealed that the Phase I response was similar in all the 5'-AMP treated mice, from the lowest to the highest dosages and is independent of T_b. For most mice to enter DH under the experimental condition used, a minimum dose of 0.25 mg/gw was required. Thus, our studies revealed that once the minimum dose of 5'-AMP is reached, giving a higher dose does not extend the time in DH. Therefore, it was concluded that the 5'-AMP injection of 0.25 mg/gw or more initiates DH, but does not control the length of time in that state. However, as shown previously in Figures 2a and 2b, for mice given the same dose of 5'-AMP, the T_a plays an important role in the length of time in DH. Of the mice given 0.5 mg/gw 5'-AMP, the group in the 15 °C environment stayed in the state for lengths ranging from 2 to 8 hours, whereas the group in the 23 °C environment only lasted less than 2 hours.

Higher T_a causes more rapid recovery from DH

The studies above showed that T_a is important in allowing the animal to cool, but it was important to test the effect of T_a on how quickly animals recover from DH. Mice were injected with 0.5 mg/gw 5'-AMP and placed in the 15°C metabolic chamber until their T_b reached about 16°C. Then, each group was placed in a different T_a, and the T_b was monitored until the animals had fully recovered to euthermia (Figure 5).

Figure 5: Arousal from DH and the rise in T_b of mice maintained at various T_a values. (*n*=4) This research was originally published in The Journal of Biological Chemistry. Daniels IS, Zhang J, O'Brien WG, Tao Z, Miki T, Zhao Z, Blackburn MR, Lee CC. Title. J Biol Chem. 2010; 285:20716-20723. © the American Society for Biochemistry and Molecular Biology.
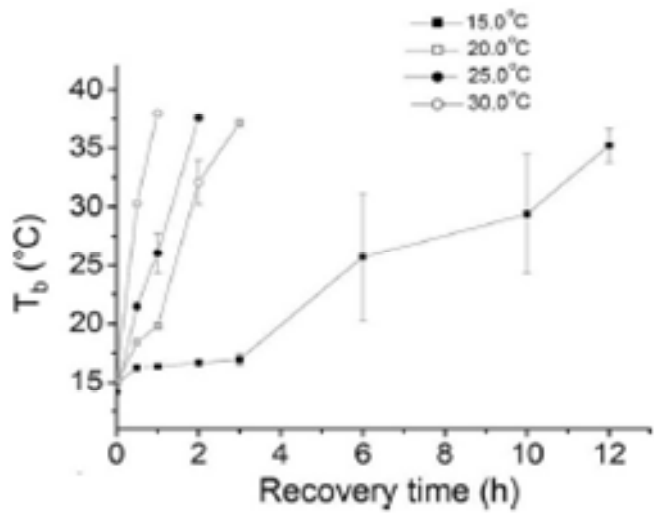
Mice kept in 15°C T_a stayed in DH the longest. As the T_a increased, the recovery from DH was correspondingly faster. These data demonstrate that the T_a is important in modulating the length of time it takes for arousal. However, the fact that once the minimum dose of 5'-AMP is reached, the dose of the 5'-AMP does not extend the length of time in DH, and the variability of length in DH, shows there are still factors that control arousal that remain unknown. This is supported by observations that giving the animals a second injection of 5'-AMP failed to prolong DH, and instead it led to increased mortality. In addition, further reduction of T_b to 14°C or lower led to increased mortality.

In summary, the Phase I response of a rapid and dramatic decline in VO_2 after 5'-AMP injection does not depend on the T_a or the T_b of the animals. However, the Phase II response, which is a more gradual decline in VO_2, accompanied by a parallel decline in T_b, is controlled by the T_a. During Phase II the T_a mediates the extent to which the animal will cool, as the body heat is transferred from a warm to a cooler state. However, the length of time until arousal varies for animals that have already entered DH and are maintained at the same T_a. Increased T_a enhanced the arousal and recovery rate from DH.

Other species have successfully been induced into DH.

It was important to determine whether the effect of 5'-AMP would translate to larger mammals because it could possibly be used for therapeutic purposes in humans in the future. Also, it is easier to make some physiological measurements in larger mammals.

Induction of a rat into DH

To test whether the effect of 5'-AMP will work in larger rodents, large male Sprague-Dawley rats, weighing 450 – 550g, were injected with 0.5 mg/gw 5'-AMP *i.p.*, and cooled initially at 4°C T_a. After approximately 2 hours, the animals entered DH when the animal's ability to right itself when laid on its side was no longer possible, with a corresponding T_b of 18 - 20°C. Transferred to 15°C T_a, the rats were able to maintain DH for 6 hours, after which they were gradually rewarmed to euthermia (Figure 6a). Thus, my studies showed that another species of rodent displayed a similar response to 5'-AMP – induced deep hypometabolism.

Induction of a dog into DH

To determine if the DH model works in another species of mammals, a beagle mix dog, weighing approximately 5 kg, was given 1.5 mg/g 5'-AMP via *i.p.* injection, and placed initially in a 4°C environment (Figure 6b). After 3 hours the animal entered the DH state, with a T_b of 22°C. It was transferred to an 18°C environment and it maintained a T_b of 21-22°C for 8 hours, after which it was gradually rewarmed to initiate arousal. After about 8 more hours it had returned to euthermia. These findings demonstrated that a larger species, the dog, is able to enter 5'-AMP – induced deep hypometabolism.

Figure 6: Rat and dog induced into DH by injection with 5'-AMP and cooling. a, A representative profile of a 450 g male Sprague-Dawley rat was injected *i.p.* with 0.5 mg/gw 5'-AMP and cooled in a 4 °C T_a for 2 hours until the animal had entered DH with a T_b of ~18 °C. Then it was maintained in 15 °C T_a with a T_b of 18-20 °C for 6 hours, and then gradually rewarmed to induce arousal. b, A representative profile of a ~5 kg beagle mixed breed dog injected *i.p.* with 1.5 mg/gw 5'-AMP and cooled in a 4 °C T_a for 3 hours until the animal had entered DH with a T_b of ~22 °C. Then it was transferred to 18 °C T_a and its T_b remained at ~21-22 °C for 8 hours, then the animal was gradually rewarmed to induce arousal, and it returned to euthermia within 8 hours. This research was originally published in The Journal of Biological Chemistry. Daniels IS, Zhang J, O'Brien WG, Tao Z, Miki T, Zhao Z, Blackburn MR, Lee CC. Title. J Biol Chem. 2010; 285:20716-20723. © the American Society for Biochemistry and Molecular Biology.

a

5'-AMP

Rat

b

Dog
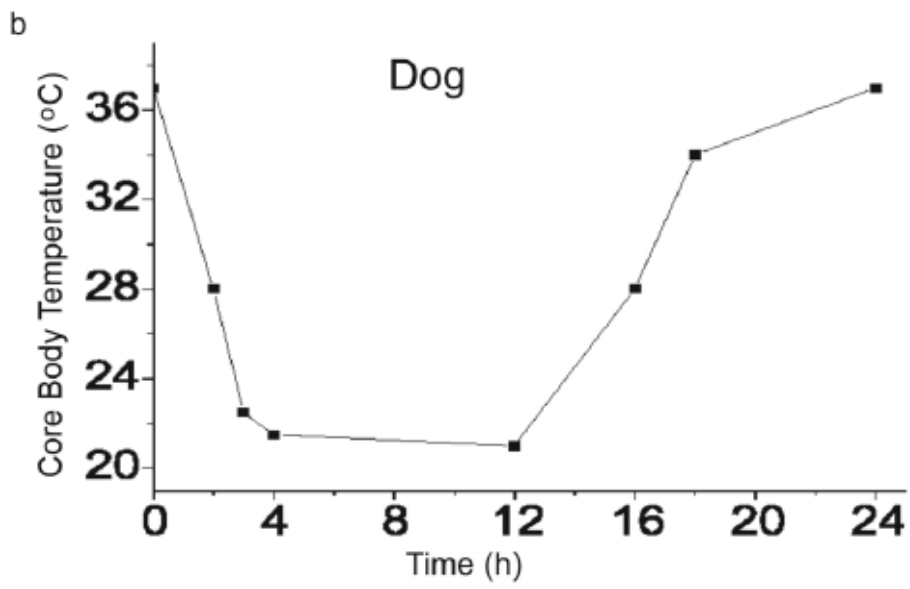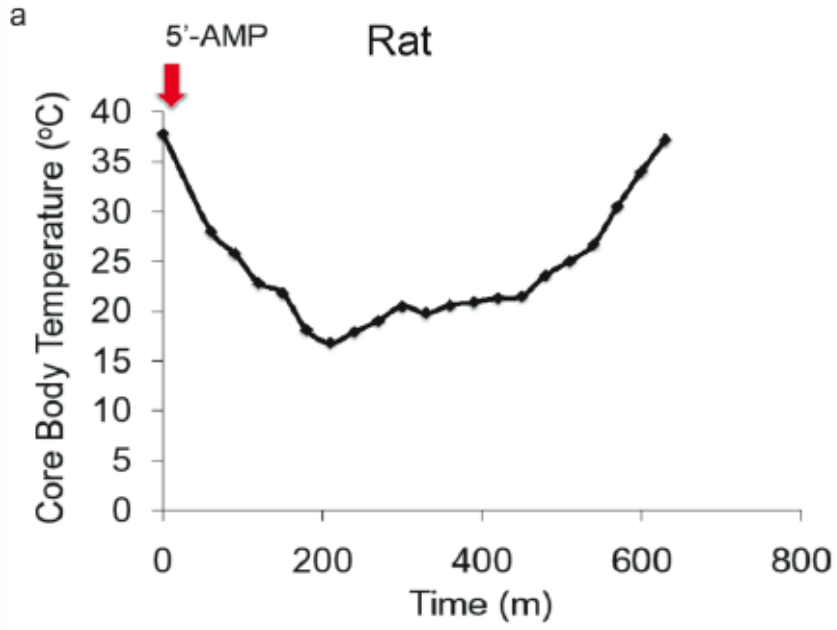
Induction of a pig into DH

The effect of 5'-AMP – induced hypometabolism was also tested in pigs because the pig physiology is similar enough to that of humans to be valuable models for preclinical testing of drugs and surgical methods (34). A female Yucatan micro-mini pig weighing 27 kg was injected with 1.0 g/kg 5'-AMP, *i.v.,* through a catheter inserted in the ear, and cooled with 10°C cooling blankets (Figure 7). The animal was maintained on 2% inhaled isoflurane anesthesia for approximately 20 minutes before 5'-AMP injection, and then 1% isoflurane throughout the cooling process. T_b was measured by esophageal probe. The animal began to slightly shiver 100 minutes after injection, at which point T_b was 31°C. Anesthesia and cooling were stopped, but T_b continued to decrease despite the shivering, reaching a nadir of 29.6°C. Gradually the animal's T_b rose and it returned to euthermia and normal behaviors after several hours. While the pig was able to be cooled after injection of 5'-AMP, anesthesia had to be used according to the institution animal welfare guidelines, so it was not possible to separate the effects of the anesthesia from the effects of the 5'-AMP.

Figure 7: Induction of a pig into DH. A 27 kg Yucatan micro-mini pig was administered 5'-AMP (1.0 mg/gw) intravenously over a 20 minute period (injection time indicated in blue shading) under 2% isoflurane anesthesia and placed between 10°C cooling blankets. Cooling blankets and anesthesia were removed at 100 min at onset of shivering but T_b continued to decline to a nadir of 29.6°C.
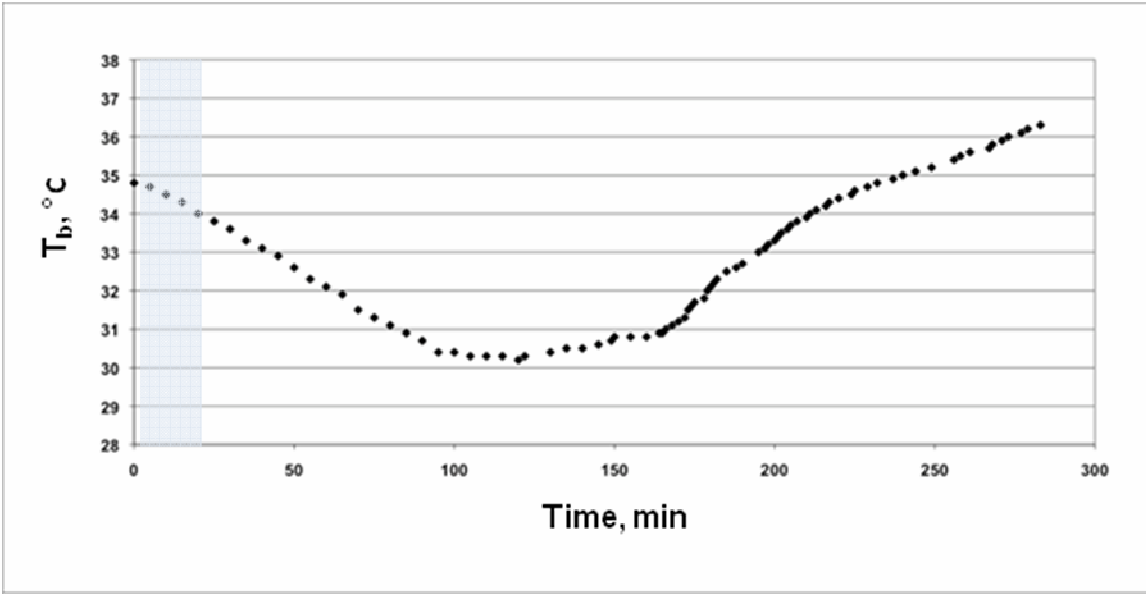
In summary, 5'-AMP injection induces a hypometabolic state that is moderated by T_a. There are two distinct phases of response after injection: a Phase I response characterized by a rapid, dramatic decrease in VO_2 with not much decrease in T_b, and a Phase II response characterized by a gradual decline in VO_2 and T_b that is dependent on the T_a. Once the minimum dose is reached, the dose effect of 5'-AMP on length of time in DH and reduction of VO_2 and T_b is not linear. In addition to mice, rats, a dog, and pigs were induced into DH state by 5'-AMP injection and cooling, and these data serve as proof of principle that the model works in larger mammalian species. Therefore, the mechanisms for inducing the DH state are shared in other species. Also, it suggests the model could potentially translate to humans for clinical applications such as therapeutic hypothermia. Understanding the fate of the injected 5'-AMP and the mechanisms that initiate the DH state is important for future applications.

Chapter 4

Investigation of the role of 5'-AMP in the model of deep hypometabolism

Since 5'-AMP can be converted to other molecules outside the cell, it was important to determine whether 5'-AMP itself was initiating the model. As shown in Figure 8, 5'-AMP can be converted to adenosine outside the cell in a reaction catalyzed by 5'-ectonucleotidase, also called CD73 (14, 16). In addition, it is well-known that 5'-AMP can be phosphorylated to form ADP and ATP via adenylate kinase. The generation of 5'-AMP can come from catabolism of 3',5'-cyclic adenosine monophosphate (cAMP) by phosphodiesterase (14, 16).

Figure 8: Adenosine metabolism and receptor signaling outside and inside the cell
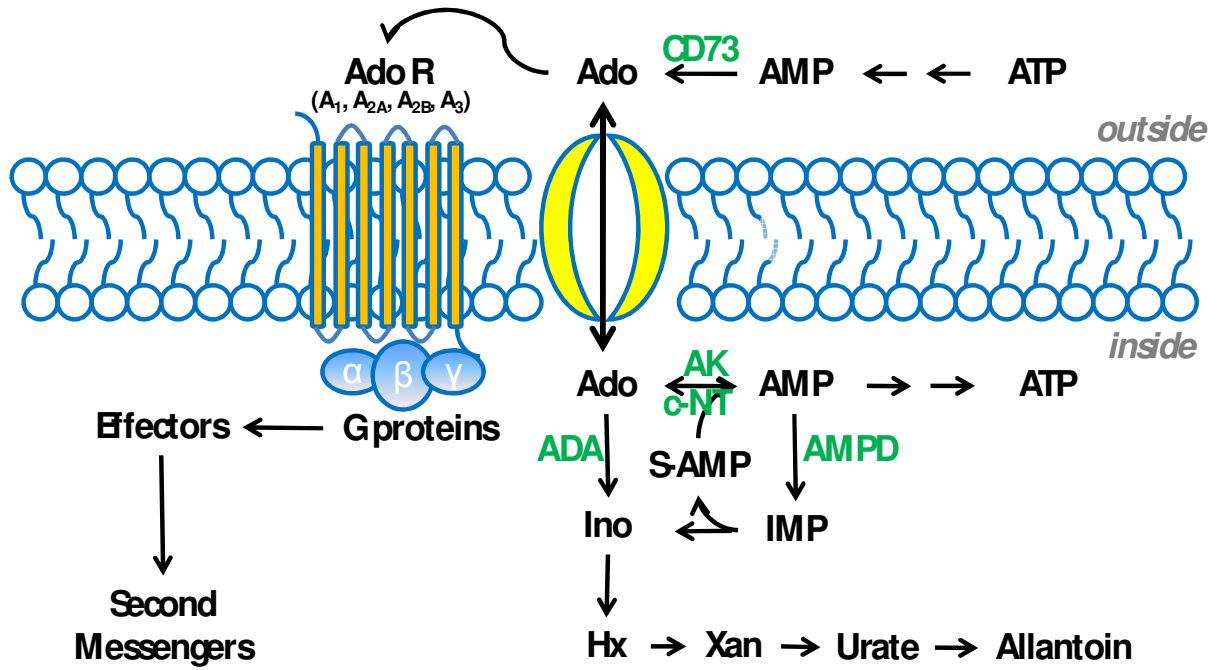
Can different nucleotides initiate the DH model?

Other mononucleotides were tested to investigate whether the hypometabolic effects were specific to 5'-AMP. Mice were injected with 0.5 mg/gw of either 5'-AMP, 5'-cytidine monophosphate (5'-CMP), or 5'-guanosine monophosphate (5'-GMP) and placed in the metabolic chamber at 15°C (Figure 9). The mouse given 5'-AMP experienced the Phase I and Phase II responses, and remained in DH for almost 10 hours. In contrast, neither the 5'-CMP nor the 5'-GMP injected animals had any significant change in VO_2, and their T_b remained euthermic.

Figure 9: Comparison of VO$_2$ levels in mice given 5'-AMP, 5'-CMP, or 5'-GMP. Each mouse was injected with 0.5 mg/gw of either nucleotide. This research was originally published in The Journal of Biological Chemistry. Daniels IS, Zhang J, O'Brien WG, Tao Z, Miki T, Zhao Z, Blackburn MR, Lee CC. Title. J Biol Chem. 2010; 285:20716-20723. © the American Society for Biochemistry and Molecular Biology.
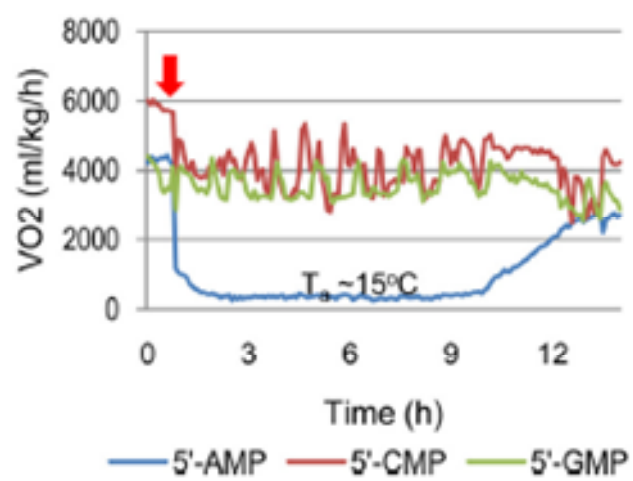
To test the effect of the other adenine nucleotides, mice were given 0.5 mg/gw ATP or cAMP, and response was compared to 5'-AMP injection. The animals did have a response, but it took much longer for the drug to take effect compared to the mice given 5'-AMP (Figures 10,11). The ATP-injected mouse Phase I response was slower than in the 5'-AMP-injected animal. The VO_2 of the ATP-injected animal took longer to decline (Figure 10). Likewise, the cAMP-injected mouse had a kinetic rate similar to ATP in its Phase I response which is much slower than that displayed by 5'-AMP (Figure 11). The VO_2 of the cAMP-injected animal also took longer to decline. In addition, other investigators have found that injection of 0.4 mg/gw ADP and ATP had similar effect to what we found with ATP and cAMP (35). These results suggest that conversion of cAMP, ADP and ATP to 5'-AMP is required to have an effect.

Figure 10: Injection of 5'-ATP results in slower Phase I response than 5'-AMP. VO_2 and T_b were measured simultaneously in mice given 0.5 mg/gw 5'-AMP or 5'-ATP in individual cages in metabolic chamber at 15°C. Red arrow indicates injection time. a, VO_2 b, T_b c, high resolution plot of VO_2 from part a. Note the difference in Phase I response. Time between sampling points is 3 min.
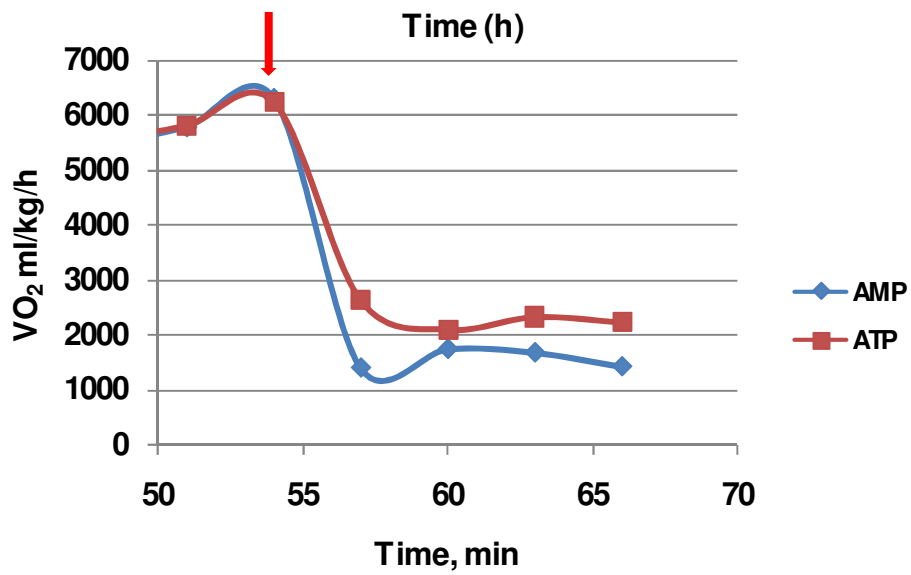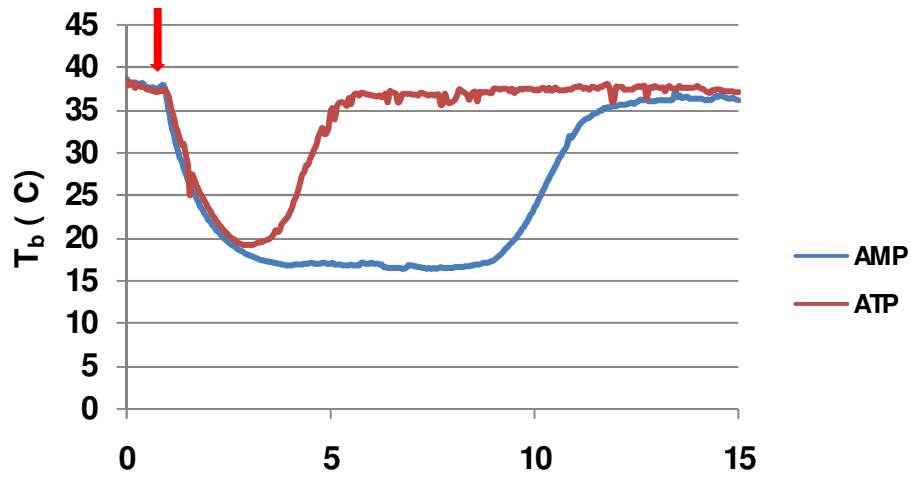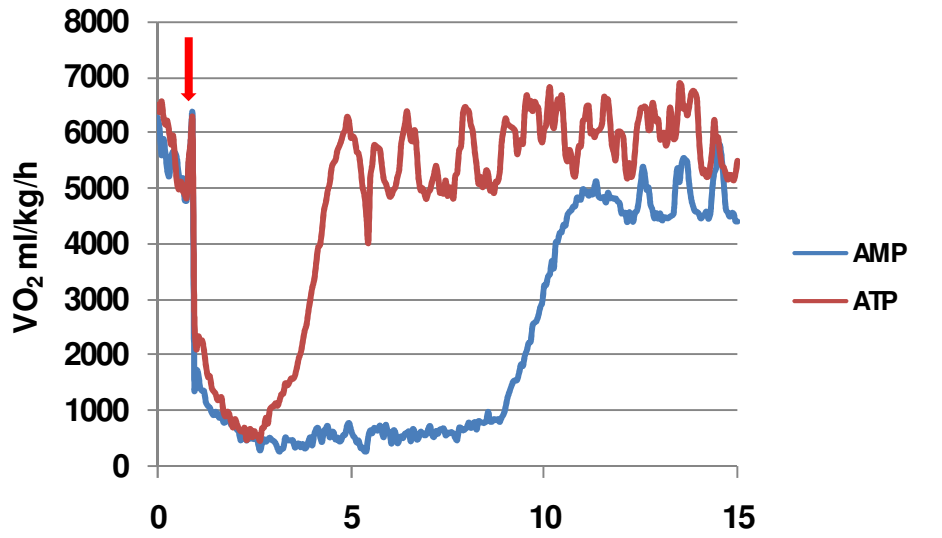
Figure 11: Injection of cAMP results in slower Phase I response than 5'-AMP
a, VO_2 was measured in mice treated with 5'-AMP or 3',5'-cyclic AMP (cAMP), (0.5 mg/gw). The cAMP treated mouse displays slower Phase I response 5'-AMP treated mouse. The cAMP treated mouse has an aborted Phase II response. The boxed area is shown in higher resolution in b, with 5 min sampling time. This research was originally published in The Journal of Biological Chemistry. Daniels IS, Zhang J, O'Brien WG, Tao Z, Miki T, Zhao Z, Blackburn MR, Lee CC. Title. J Biol Chem. 2010; 285:20716-20723. © the American Society for Biochemistry and Molecular Biology.
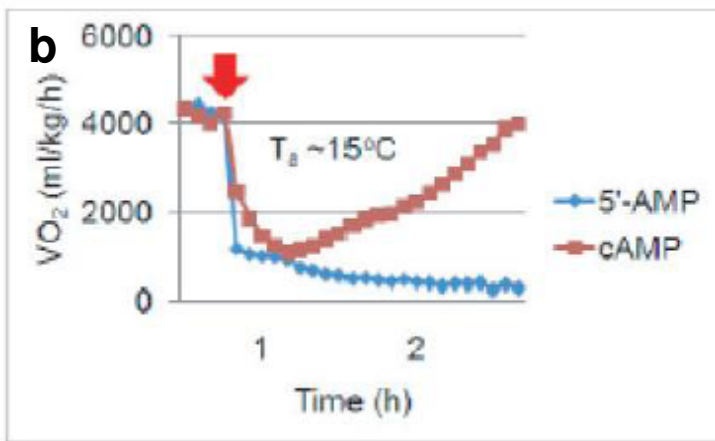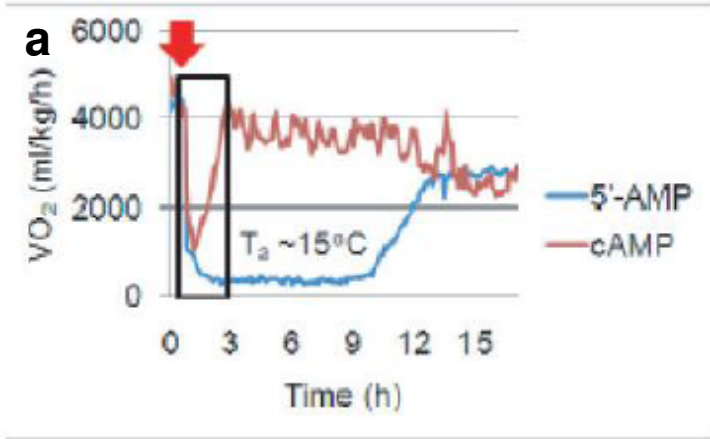
Adenosine was also tested. Mice given adenosine experienced a Phase I response, with the quick decrease in VO_2, but did not have a Phase II response, and therefore did not enter DH (Figure 12). This transient effect of adenosine is not surprising as its half-life is less than 10 seconds in the serum (36). The result suggests adenosine is quickly metabolized before it can be phosphorylated into enough 5'-AMP to cause a Phase II response.

Figure 12: Injection of adenosine results in a Phase I response but an aborted Phase II response. VO_2 was measured in mice treated with saline, 5'-AMP (0.5 mg/gw) or adenosine (0.5 ml of 10 mg/ml) in 15°C T_a. This research was originally published in The Journal of Biological Chemistry. Daniels IS, Zhang J, O'Brien WG, Tao Z, Miki T, Zhao Z, Blackburn MR, Lee CC. Title. J Biol Chem. 2010; 285:20716-20723. © the American Society for Biochemistry and Molecular Biology.
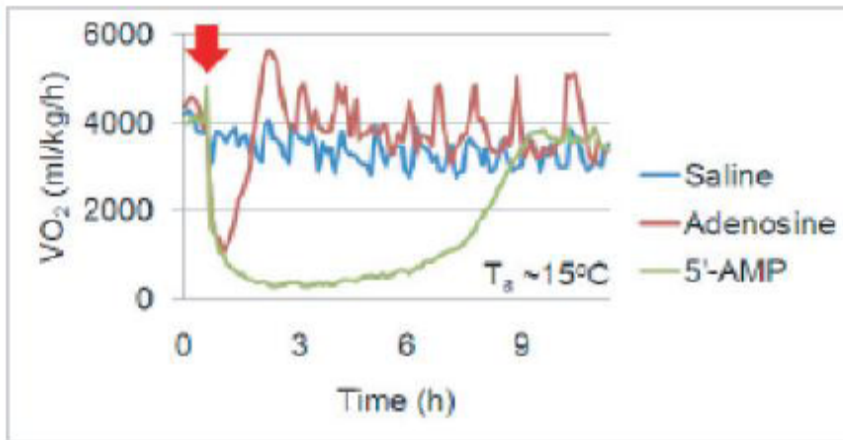
Loss of CD73 did not block 5'-AMP induction of DH

The enzymes and receptors involved in adenylate metabolism and signaling are well studied, so they are useful tools in dissecting the fate of the injected 5'-AMP. Outside the cell, 5'-AMP is dephosphorylated by the cell membrane anchored enzyme 5'-ectonucleotidase/CD73 to form adenosine (Figure 8). Thus, if conversion of 5'-AMP to adenosine outside the cell is required to initiate DH, then CD73 deficient mice would be highly resistant to DH induced by 5'-AMP. The metabolic responses were compared between wild-type and CD73 deficient mice given 5'-AMP and cooled. If conversion of 5'-AMP to adenosine outside the cell is essential to initiate DH, then the CD73 deficient mice would be more resistant to 5'-AMP induction of DH. The mice were injected with 0.5 mg/gw 5'-AMP and placed in a 15°C metabolic chamber (Figure 13a). Interestingly, the CD73 deficient mice showed a similar response to the wild-type mice, with Phase I and Phase II responses, and stayed in DH for several hours. This result suggests that the dephosphorylation of 5'-AMP to adenosine by CD73 is not necessary to induce the DH state.

Another experiment was performed to determine if the CD73 deficient mice would respond differently to a lower dose of 5'-AMP (Figure 13b). Mice lacking the enzyme CD73 would effectively be receiving a higher dose of 5'-AMP than the wild-type mice because the 5'-AMP is not being converted to adenosine. The dose of 5'-AMP, 0.125 mg/gw, was chosen since it is not completely effective in initiating DH in wild-type mice. Mice of each group ($n = 12$) were injected, and placed in a 4°C T_a for one hour, and then T_b was measured rectally. Although a few of the wild-type

mice did cool, the majority did not reach DH. In contrast, the majority of the CD73 deficient mice entered DH. The results from this experiment demonstrate that lack of the CD73 enzyme makes a lower dose of 5'-AMP more effective.

Loss of adenosine receptors did not block 5'-AMP induction of DH

As part of analyzing the role of 5'-AMP conversion to adenosine outside the cell, it was important to determine whether adenosine receptor signaling is necessary to induce DH. Adenosine receptors have been shown to be involved in thermoregulation (37). The reaction of wild-type mice to injection of saline or 5'-AMP was compared to mice lacking either A_1, A_{2A}, A_{2B} or A_3 adenosine receptor (Figure 13c). Mice were given saline or 0.5 mg/gw 5'-AMP and then placed in a 4°C T_a for one hour.

Figure 13: Loss of adenosine receptors or 5'-ectonucleotidase deficiency does not block DH induced by 5'-AMP injection. a, the VO_2 profiles of ectonucleotidase/CD73-deficient (*n*=2) and wild-type mice following 5'-AMP (0.5 mg/gw) administration. b, individual T_b of ectonucleotidase/CD73-deficient and wild-type mice (*n*=12) after 1h at 4°C T_a with injection of 0.125 mg/gw 5'-AMP. C, top, T_b time course of mice, (*n*=4) with the adenosine receptor genotype $A_1^{-/-}$, $A_{2A}^{-/-}$, $A_{2B}^{-/-}$, or $A_3^{-/-}$ or wild-type were given 0.5 mg/g 5'-AMP after 1 h at 4°C T_a. bottom, T_b of mice of the same genotype given saline after 1 h at 4°C T_a. Error bars, S.E.M. This research was originally published in The Journal of Biological Chemistry. Daniels IS, Zhang J, O'Brien WG, Tao Z, Miki T, Zhao Z, Blackburn MR, Lee CC. Title. J Biol Chem. 2010; 285:20716-20723. © the American Society for Biochemistry and Molecular Biology.

a.

b.

c.
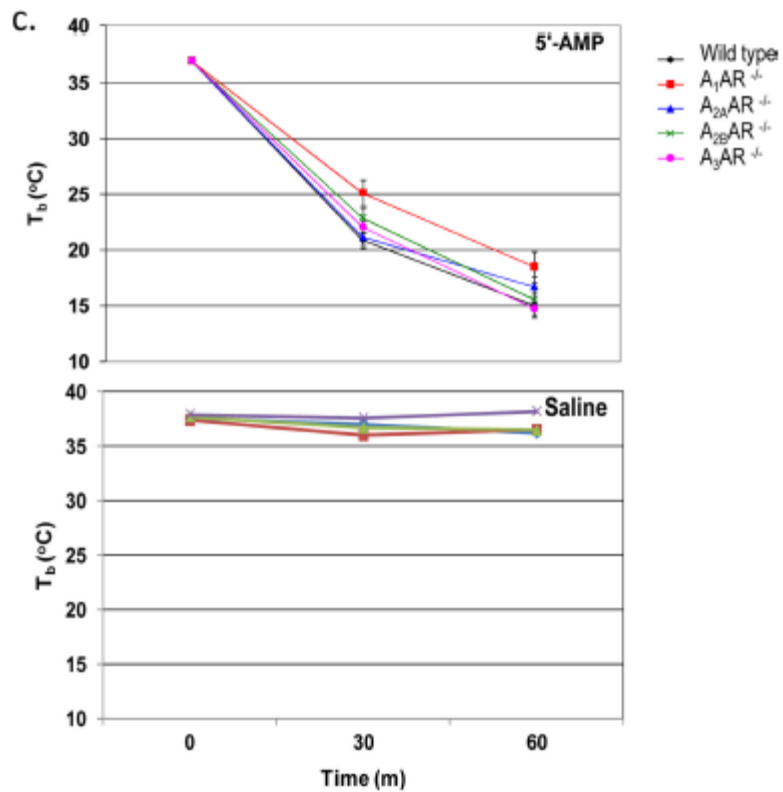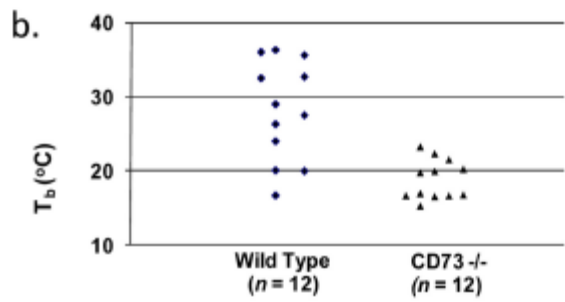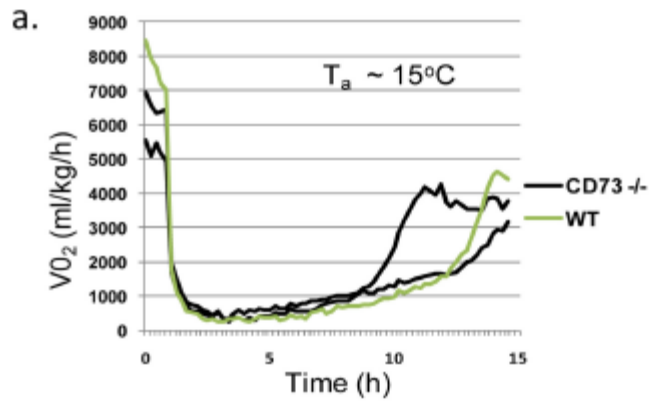
Body temperature was measured rectally before injection, at 30 minutes and at one hour. All the wild-type and adenosine receptor deficient mice reacted similarly. The animals maintained body temperature after injection with saline. In contrast, the 5'-AMP injected animals all cooled to a body temperature of about $17°C$, and had entered DH by one hour post injection. The rate of cooling was similar between all groups. Additionally, the VO_2 response of the adenosine receptor deficient mice was measured in the metabolic chamber (Figure 14). Wild-type and adenosine receptor deficient mice were placed in the metabolic chamber at $15°C$ and treated with 0.5 mg/gw 5'-AMP. All the adenosine receptor deficient mice behaved similarly to the wild-type mice. There was a rapid decline in VO_2 for the Phase I response, and then a slower decline in VO_2 until the animals reached DH. They remained in that state for several hours before arousal and recovery to euthermia and normal VO_2. These results demonstrate that no single adenosine receptor is required to initiate the effect. This is important because it suggests that adenosine signaling is not required for inducing the effect.

Figure 14: Wild-Type and adenosine receptor deficient mice have similar metabolic rate response to 5'-AMP injection and cooling at 15°C. Each line represents the VO_2 profile of one adenosine receptor genotype $A_1^{-/-}$, $A_{2A}^{-/-}$, $A_{2B}^{-/-}$, or $A_3^{-/-}$ or wild-type mouse. Arrow indicates time of injection with 5'-AMP (0.5 mg/gw). Phase 1 (PI) and Phase II (PII) responses are indicated.
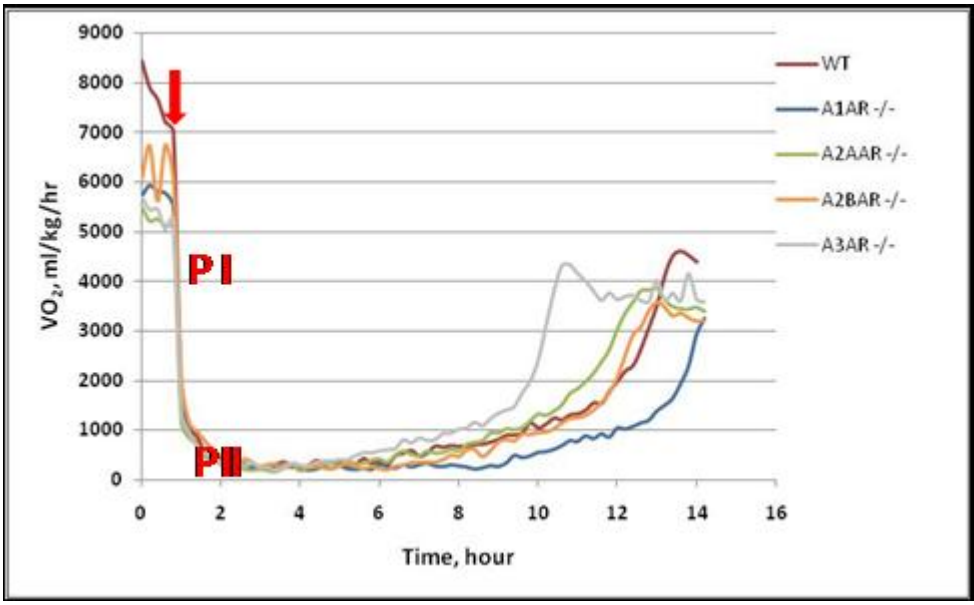
Rapid decrease in heart rate is not required to initiate DH

One of the striking physiological changes observed in animals injected with 5'-AMP is a rapid and dramatic decrease in heart rate. The A_1 adenosine receptor is known to mediate heart rate and vasodilation (37). Stimulating the A_1 adenosine receptor decreases heart rate by decreasing conduction of electrical impulses and suppressing pacemaker cell function (38).

To determine whether adenosine receptor control of heart rate plays a role in inducing DH, wild-type mice and mice deficient in A_1, A_{2A}, A_{2B} or A_3 adenosine receptor were injected with 5'-AMP, placed in a 22°C environment, and heart rate and T_b were monitored under isoflurane anesthesia for one hour (Figure 15). All the mice cooled similarly, reaching a body temperature of approximately 23°C. The heart rate of the wild-type and the A_{2A}, A_{2B} and A_3 receptor deficient mice decreased rapidly, reaching approximately 200 beats per minute within 2 minutes of injection. In contrast, the heart rate of the A_1 receptor deficient mice did not show this rapid decrease. This result corresponds to the function of the A_1 adenosine receptor in mediating heart rate. Even though the A_1 receptor deficient mouse did not have the sharp decrease in heart rate after the 5'-AMP injection, it still cooled similarly to the wild-type mouse and the other adenosine receptor deficient mice. This shows that the adenosine receptor signaling influence on heart rate is not required to induce the model, and also that the rapid decrease in heart rate itself is an effect, and not a cause.

Figure 15: Rapid decrease in heart rate is not essential to induce DH. One each of wild-type, A1, A2A, A2B, and A3 adenosine receptor deficient mice were injected with 0.5 mg/gw 5'-AMP at 22°C T_a. Heart rate and T_b were measured simultaneously. Data from Dr. Zhenyin Tao, unpublished observation.
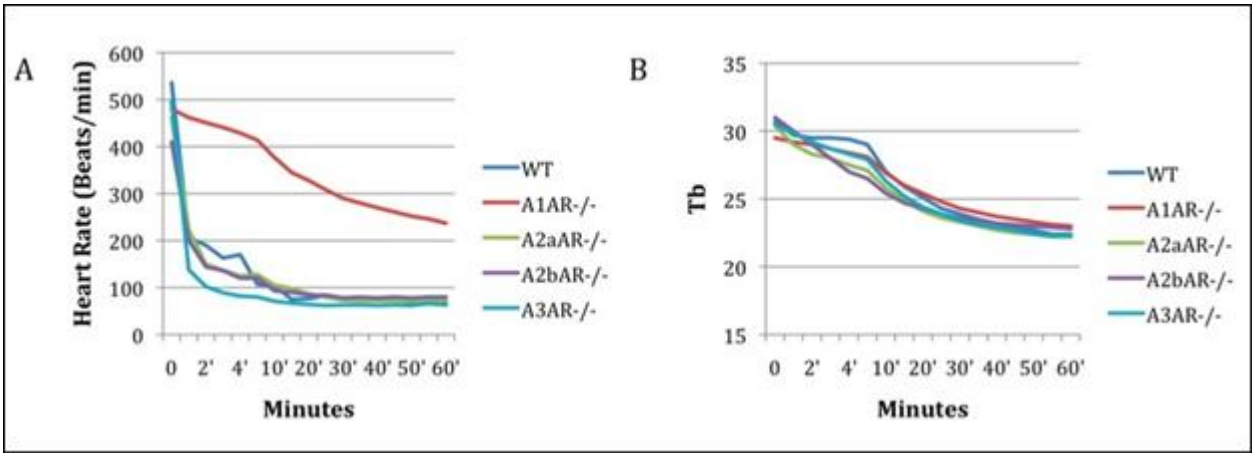
In summary, the results from the CD73 deficient mice experiments show that dephosphorylation of 5'-AMP to adenosine outside the cell is not required for the initiation of DH. The loss of adenosine receptors did not affect the ability of 5'-AMP to initiate the hypometabolic response. Adenosine can initiate the Phase I response but its effect is rather short lived. The loss of A_1 adenosine receptor did not block 5'-AMP - induced DH but it blocked the rapid bradycardia effects of adenosine. The kinetics of ATP and cAMP are much slower than that initiated by 5'-AMP in the induction of DH. Other nucleotides including 5'-CMP and 5'-GMP are not effective. The results suggested that 5'-AMP itself may be initiating the DH model. To gain more insight into the mechanisms involved, we measured metabolic and biochemical parameters.

Chapter 5

The erythrocyte is the site of initiation for the 5'-AMP – induced model of deep hypometabolism

The results from the experiments with the CD73 deficient and adenosine receptor deficient mice demonstrated that dephosphorylation of 5'-AMP to adenosine and adenosine receptors signaling was not essential to induce the deep hypometabolism model. Further biochemical analysis was needed to determine the fate of the 5'-AMP. We undertook studies to determine the metabolic and biochemical changes that occur after 5'-AMP injection.

The serum of mice in DH contains elevated purine catabolic products

A metabolomics study gave a detailed overview of the metabolic status of mice in DH. Serum was analyzed from mice before injection, 3 hours into DH, at the arousal stage, and early in their recovery. Analysis incorporated liquid and gas chromatography and mass spectrometry to determine the metabolites in the samples and calculate relative fold difference from the euthermic state, and was carried out by a commercial service company (Metabolon, Research Triangle Park, NC). Compared to the euthermic level, the 5'-AMP level in the serum of mice in deep hypometabolism and at the arousal stage was increased only by 1.2 - 1.5 fold. This suggests that much of the injected 5'-AMP had already been catabolized by the time the mice were in DH. Further evidence of the 5'-AMP catabolism came from the results that showed levels of several of the purine catabolites, such as inosine, xanthine, xanthosine, hypoxanthine, urate, and allantoin had greatly increased by DH (Table 1). Analysis of serum metabolites of mice in early recovery showed that the purine catabolites had generally returned to the levels seen in mice before injection, with the exception of allantoin, the final product in the purine catabolic pathway in mice. During the deep hypometabolic state, there was about a

2 fold increase in ADP levels, whereas adenosine levels were lower than euthermic

state. The metabolite measurements suggest that the 5'-AMP is being primarily

catabolized by the AMP deaminase rather than through the adenosine deaminase

pathway (Table 1).

Table 1 Metabolomics analysis shows significant alternation in relative levels of purine intermediates in serum. This research was originally published in The Journal of Biological Chemistry. Daniels IS, Zhang J, O'Brien WG, Tao Z, Miki T, Zhao Z, Blackburn MR, Lee CC. Title. J Biol Chem. 2010; 285:20716-20723. © the American Society for Biochemistry and Molecular Biology.

Relative levels of purine intermediates in serum that showed significant alteration during euthermia, deep hypometabolism, arousal, and early recovery

For each group, the relative quantization value of each metabolite is the average obtained from seven mice. For each of the metabolites, the average euthermia control value is arbitrarily set at 1. The -fold change in DH, arousal, and early recovery is relative to the value obtained for euthermia. The probability that the changes were due to random factors is quantified by the p values, and the false positive rate is quantified by q values of t tests that are shown in italic type. (Note that for the data points with missing values, no acceptable measurement for that compound was obtained for the group.)

Altered purine metabolites ($n = 7$)	DH/Euthermia			Arousal/Euthermia			Early recovery/Euthermia		
	-Fold change	p value	q value	-Fold change	p value	q value	-Fold change	p value	q value
Xanthine	8.83	0.000	0.001	4.97	0.012	0.007	1.13	0.356	0.127
Xanthosine	11.8	0.000	0.000	2.82	0.004	0.003	1.03	0.793	0.227
Hypoxanthine	8.69	0.004	0.005	3.07	0.033	0.017			
Inosine	4.91	0.026	0.021	1.30	0.351	0.115			
Adenosine	0.66	0.004	0.005	0.41	0.033	0.017	0.61	0.523	0.166
5'-AMP	1.21	0.026	0.021	1.44	0.351	0.115	0.92	0.587	0.178
ADP	1.79	0.021	0.019	2.02	0.004	0.003	0.95	0.807	0.228
Urate	3.3	0.001	0.001	2.70	0.002	0.002	1.57	0.144	0.064
Allantoin	15.3	0.000	0.000	18.16	0.000	0.000	13.44	0.000	0.000

Serum and erythrocytes of mice in DH have elevated 2,3-bisphosphoglycerate

Another interesting finding from the metabolomics analysis is that there was a large increase in 2,3-bisphosphoglycerate (2,3-BPG) in the mice in DH compared to mice preinjection (Table 2). 2,3-BPG is synthesized from 1,3-BPG in the erythrocyte and in the placenta, catalyzed by the enzyme bisphosphoglycerate mutase. This enzyme is only found in erythrocytes and placenta, so the increase in 2,3-BPG during DH suggested that the erythrocyte is implicated in the model. To further investigate the timing of the increase in 2,3-BPG after 5'-AMP injection, an experiment was performed in which the 2,3-BPG levels were measured in erythrocyte samples isolated from blood taken from mice over a time course before and after 5'-AMP injection (Figure 16). The 2,3-BPG levels had significantly increased by the first sampling 10 minutes after injection, and continued to rise during the following 30 minutes. However, by arousal state, the levels of 2,3-BPG had returned to preinjection levels. These results suggested the possibility that the erythrocyte is involved in the underlying mechanism of deep hypometabolism induced by 5'-AMP.

Table 2: Metabolomics analysis shows 3.57-fold increase in 2,3-BPG in serum of mice in DH compared to euthermia

Altered Glycolytic Metabolites (n=7)	DH/Euthermia			Arousal/Euthermia			Early Recovery/Euthermia		
	Fold change	p value	q value	Fold change	p value	q value	Fold change	p value	q value
Glucose	2.45	0.003	0.004	2.06	0.005	0.003	1.89	0.200	0.083
Glucose 6-phosphate	3.64	0.001	0.001	3.82	0.001	0.001	1.27	0.816	0.229
Fructose 6-phosphate	2.38	0.020	0.018	2.40	0.018	0.010	1.22	0.481	0.157
3-Phosphoglycerate	2.32	0.007	0.008	2.95	0.011	0.007	1.27	0.718	0.210
2,3-Bisphosphoglycerate	3.57	0.060	0.040	4.05	0.020	0.011			
Phosphoenolpyruvate	2.22	0.004	0.005	2.50	0.003	0.003	1.31	0.271	0.105
Pyruvate	0.09	0.000	0.000	0.08	0.000	0.000	0.56	0.003	0.005
Lactate	0.26	0.000	0.000	0.32	0.001	0.001	0.71	0.025	0.017

Figure 16: 2,3-BPG levels rise in the erythrocytes (RBC) of mice after 5'-AMP injection and then return to pretreatment levels by arousal from DH. $n = 6$, error bars indicate +/- S.E.M, $p < 0.05$. This research was originally published in The Journal of Biological Chemistry. Daniels IS, Zhang J, O'Brien WG, Tao Z, Miki T, Zhao Z, Blackburn MR, Lee CC. Title. J Biol Chem. 2010; 285:20716-20723. © the American Society for Biochemistry and Molecular Biology.

a

2,3 BPG in RBC (umol/gHb)

Time after 5'-AMP administration (m)
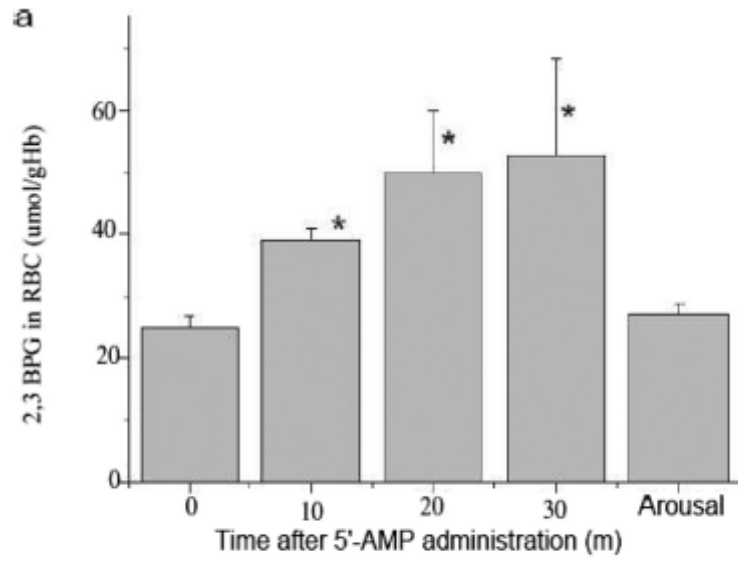
After ^{14}C-AMP injection in vivo, ^{14}C signal is highest in blood, heart, lung and kidney

A literature search revealed a study in which mice were injected with ^{11}C-AMP and then the ^{11}C signal was traced to primarily lungs, blood and heart. The authors did not perfuse the tissues, so some of the signals in lung and heart may have come from blood in these organs (39). The authors observed that very little of the ^{11}C signal crossed the blood brain barrier. In the study, they further demonstrated that the ^{11}C-AMP was rapidly taken up by erythrocytes and was first converted to ADP and then ATP. In addition, they showed that uptake of ^{11}C-AMP by the blood, unlike in the lungs, was not inhibited by dipyridamole, an inhibitor of adenosine uptake by the cells. The authors also observed that kidney and bladder were critical organs for the ^{11}C signal, indicating that the ^{11}C-AMP is metabolized and cleared through the urinary system. To replicate these studies, blood and perfused tissues were collected from a female C57Bl/6 mouse 5 minutes after injection with ^{14}C-AMP (Figure 17). Samples were homogenized and then scintillation counts of ^{14}C signal were measured, normalized to protein concentration. Similar to the published results, the highest ^{14}C signal was in the blood, heart, and lung, and in addition the kidney had high counts. Consistent with published observations, there was very little ^{14}C signal in the brain, which suggests that the injected 5'-AMP did not cross the blood-brain barrier. The observation that blood had high ^{14}C signal corresponded with the results showing elevated 2,3-BPG levels in the mice given 5'-AMP, suggesting that the erythrocyte could be an important target of the metabolite.

Figure 17: ^{14}C signal is highest in blood, heart, lung and kidney after ^{14}C-AMP injection *in vivo*. Blood and tissues were collected from a wild-type C57Bl/6 female mouse 5 minutes post-injection with ^{14}C-AMP.
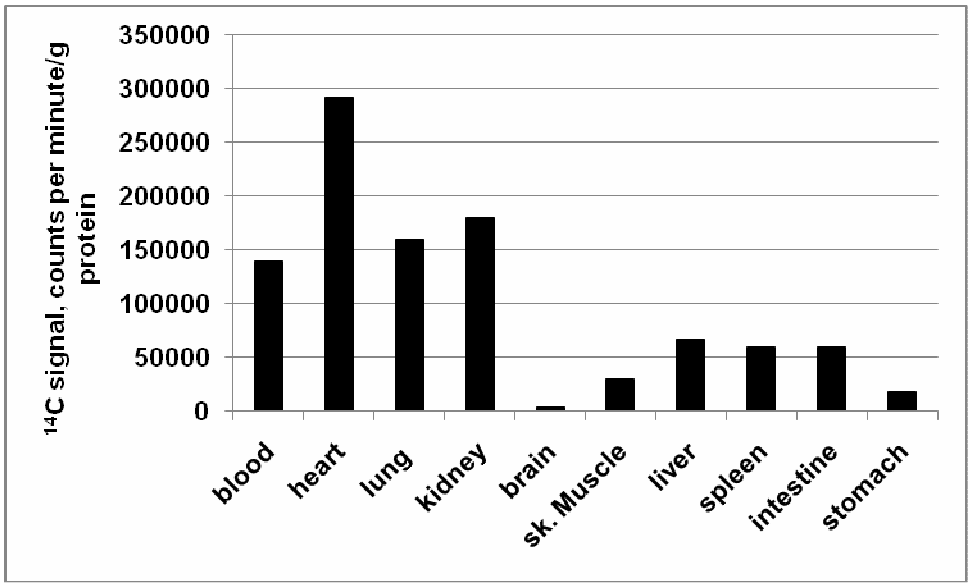
Glycolysis is slowed in the erythrocytes of mice in DH

The metabolite 2,3-BPG is a product of the glycolytic shunt in the erythrocyte. The glycolytic shunt is favored when glycolysis is slowed (16, 40). A slower rate of glycolysis would cause an increase in cellular glucose, and a decrease in lactate. Therefore, we measured glucose and lactate levels in the isolated erythrocytes of mice before 5'-AMP treatment and also during DH (Figure 18). The glucose levels of mice in DH were 3 times higher than pre-injection, whereas the lactate levels were 2 times lower. These results are consistent with a slowed glycolysis in the erythrocytes of the mice injected with 5'-AMP and this is related to the increase in 2,3-BPG. Together, these studies implicate a role for the erythrocytes in the 5'-AMP mediated hypometabolism.

Figure 18: Glucose levels increase and lactate levels decrease in the erythrocytes of mice treated with 5'-AMP. $n = 4$, error bars indicate +/- S.E.M, $p< 0.01$. This research was originally published in The Journal of Biological Chemistry. Daniels IS, Zhang J, O'Brien WG, Tao Z, Miki T, Zhao Z, Blackburn MR, Lee CC. Title. J Biol Chem. 2010; 285:20716-20723. © the American Society for Biochemistry and Molecular Biology.
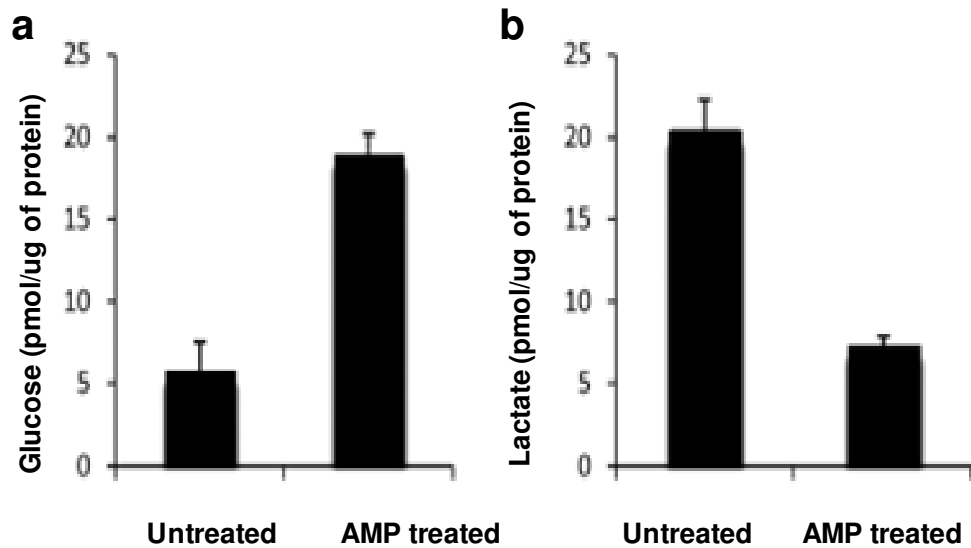
5'-AMP is taken up and metabolized in erythrocytes, favoring formation of ADP

Erythrocytes are unique in that they lack nuclei and mitochondria, therefore they rely primarily on glycolysis to make ATP and they are unable to perform *de novo* nucleotide synthesis (41, 42). Mature erythrocytes lack the enzyme adenylosuccinate synthetase, which catalyzes conversion of inosine monophosphate (IMP) to adenylosuccinate. Therefore, they are unable to complete the purine nucleotide cycle to convert IMP to AMP. They must use salvage pathways to recycle nucleotides (14, 41). Previous experiments had shown that extracellular adenosine is not required to initiate the model, but implicate that 5'-AMP itself was entering the erythrocyte. Currently there is no described transporter for 5'-AMP, but it has been reported that adenosine cyclic 3',5'-monophosphate (cAMP) and guanosine 3',5'-cyclic monophosphate (cGMP) can enter erythrocytes (43, 44). Adenosine can rapidly enter the erythrocyte (45). Previous studies have demonstrated uptake of ^{14}C-labeled adenosine into erythrocytes, and analyzed the ^{14}C-labeled products inside the erythrocyte lysate (45). Experiments were performed to determine if ^{14}C-AMP can directly enter the erythrocyte (Figure 19).

Figure 19: Uptake of ^{14}C labeled adenosine and 5'-AMP into erythrocytes isolated from wild-type mice, compared with known ^{14}C-labeled purine standards. Erythrocyte lysates were separated by thin layer chromatography. This research was originally published in The Journal of Biological Chemistry. Daniels IS, Zhang J, O'Brien WG, Tao Z, Miki T, Zhao Z, Blackburn MR, Lee CC. Title. J Biol Chem. 2010; 285:20716-20723. © the American Society for Biochemistry and Molecular Biology.
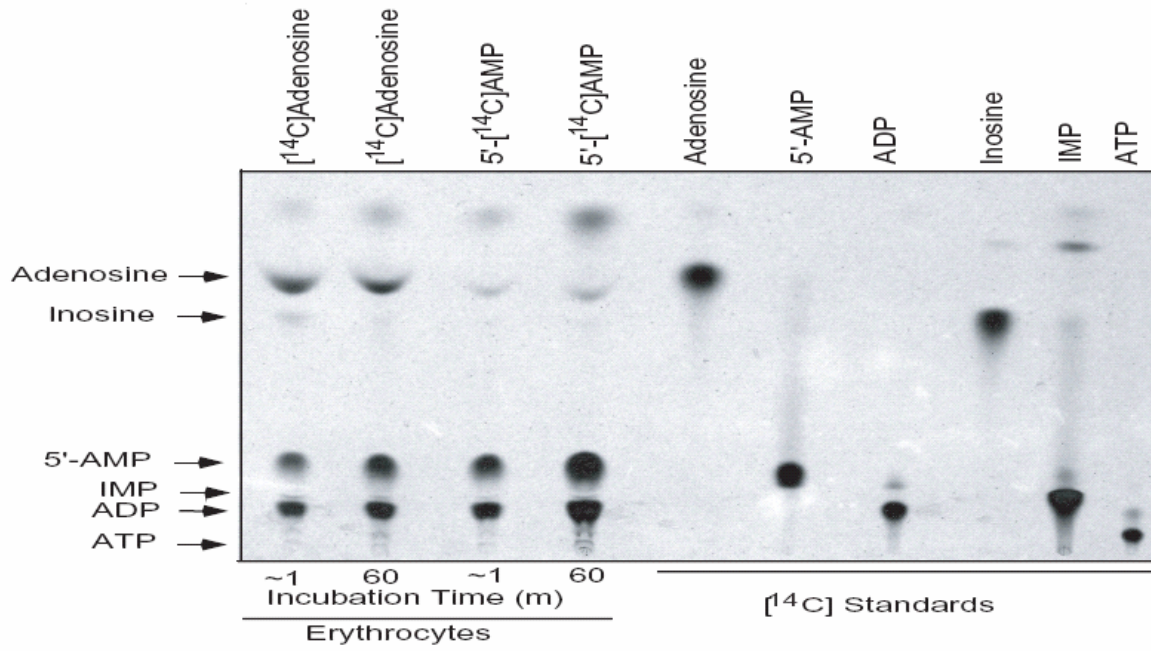
First, the experiment was performed with ^{14}C-adenosine to determine if the published results could be replicated. Isolated wild-type mouse erythrocytes were incubated with ^{14}C-adenosine over a time course up to one hour, and then washed and lysed. The contents of the cell lysate were separated by thin layer chromatography (TLC) and the radiolabeled contents were visible on an autoradiogram of the TLC plate. Radiolabeled standards were run on the TLC plate to identify the products. We observed that adenosine was taken up into the cells rapidly, consistent with the published literature. The ^{14}C-adenosine taken up into the erythrocytes mainly formed ^{14}C-AMP and ^{14}C–ADP. This suggests that inside the cell, adenosine is being phosphorylated by adenosine kinase to form AMP and then phosphorylated by adenylate kinase into ADP. When the experiment was performed with ^{14}C-AMP, rapid uptake was also observed. Product formation favored ^{14}C-ADP, and there was no detectable formation of ATP. These observations could be explained by the adenylate equilibrium AMP + ATP $\leftrightarrow$ 2 ADP. If AMP levels rise inside the cell, the adenylate equilibrium will balance this rise by converting part of the 5'-AMP into ADP by utilizing intracellular ATP. Similar outcome was observed when erythrocytes from CD73 deficient mice were used.

Analysis of the lysate contents showed uptake of ^{14}C-AMP, and formation of ADP, with trace levels of inosine and adenosine. The presence of inosine and adenosine suggests that the AMP inside the cell could be catabolized by AMP deaminase to IMP, and then IMP could be dephosphorylated to inosine by cytosolic nucleotidase. An alternative path could be AMP $\rightarrow$ adenosine by cytosolic nucleotidase, and then adenosine $\rightarrow$ inosine by adenosine deaminase. Uptake by

the CD73 deficient erythrocytes suggested the ^{14}C-AMP is likely entering the cell directly. In addition, previous studies showed that uptake of 5'-AMP by erythrocytes is not blocked by dipyridamole, unlike in the peripheral tissues (39).

ADP rises, ATP declines, and 5'-AMP is metabolized in blood of mice in DH

It was evident that 5'-AMP is taken up into the erythrocyte in the *in vitro* ^{14}C-AMP uptake experiments. However, to determine the fate of the 5'-AMP *in vivo*, an analysis of the purine nucleotides in blood was performed using HPLC. Blood extracts were analyzed from mice in euthermia, deep hypometabolism, arousal stage, and mice given a second injection of 5'-AMP during the deep hypometabolic state (Figure 20).

Figure 20: Representative HPLC chromatograms of purine products in wild-type mouse blood extracts of mice in a) euthermia, b) during DH c) spontaneous arousal, d) a mouse given a second injection of 5'-AMP (0.5 mg/gw) and sacrificed 2 hours later. This research was originally published in The Journal of Biological Chemistry. Daniels IS, Zhang J, O'Brien WG, Tao Z, Miki T, Zhao Z, Blackburn MR, Lee CC. Title. J Biol Chem. 2010; 285:20716-20723. © the American Society for Biochemistry and Molecular Biology.

a) Euthermic

c) Spontaneous Arousal

b) Deep Hypometabolism

d) 5'-AMP during DH

Retention Time (m)
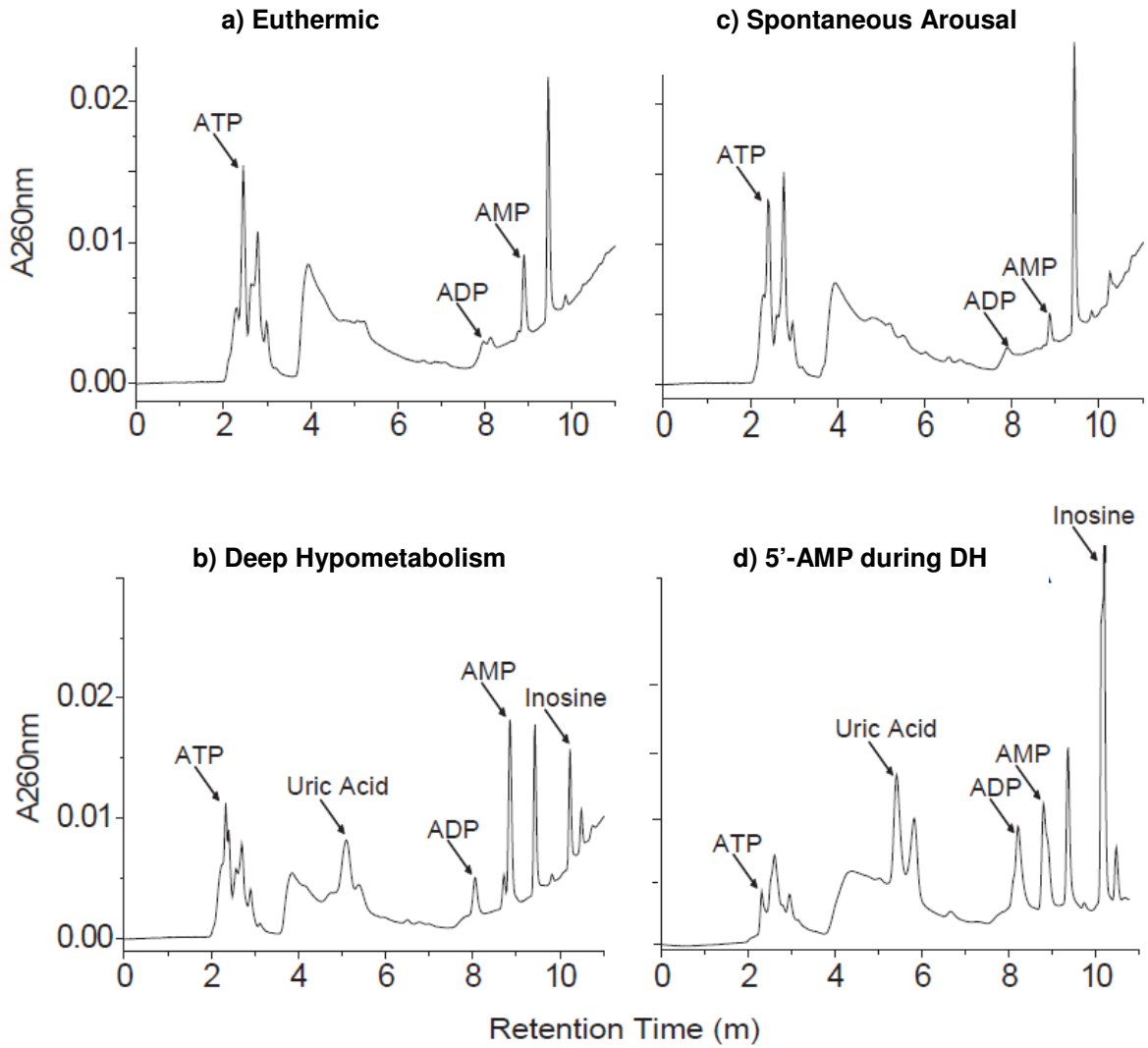
Experiments had shown that the erythrocytes of mice in DH had elevated 2,3-BPG, which is known as an allosteric regulator of the ability of hemoglobin to bind oxygen (14). Thus, high levels of 2,3-BPG would cause less oxygen to be bound to hemoglobin. When analyzed by a spectrophotometer, deoxyhemoglobin has signature peak absorbance at 760 nm, whereas oxyhemoglobin has weaker absorbance at 660 nm. Blood samples were taken 10 minutes post-injection of 0.5 mg/gw 5'-AMP or saline. Spectral analysis of samples from the treated mice showed evidence of deoxyhemoglobin at 760 nm. In contrast, samples from the untreated group had weaker absorbance at 660 nm, showing presence of more oxyhemoglobin (Figure 21). The results confirm that erythrocytes of mice treated with 5'-AMP are less able to transport oxygen to tissues.

Figure 21: Spectral absorbance of whole blood from mice treated with 5'-AMP (dashed lines) or untreated (solid lines). Blood samples were taken 10 minutes after 5'-AMP injection, *i.p.*, (0.5 mg/gw), $n = 2$. This research was originally published in The Journal of Biological Chemistry. Daniels IS, Zhang J, O'Brien WG, Tao Z, Miki T, Zhao Z, Blackburn MR, Lee CC. Title. J Biol Chem. 2010; 285:20716-20723. © the American Society for Biochemistry and Molecular Biology.
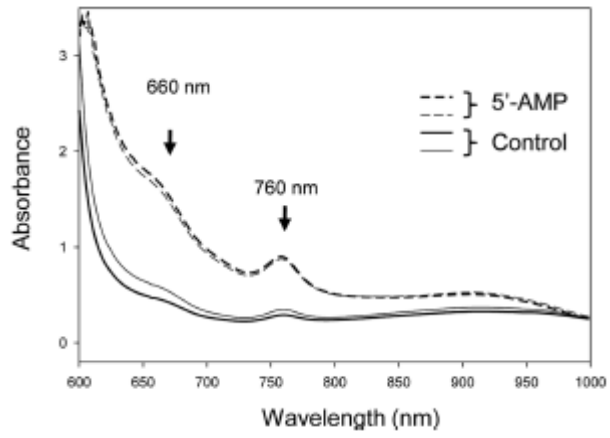
Summary of results

The metabolomics study showed an increase in 2,3-BPG in the serum of mice in DH. Erythrocytes isolated from mice treated with 5'-AMP also had increased 2,3-BPG levels, as well as increased glucose and decreased lactate levels, indicating slower rate of glycolysis. Hemoglobin oxygen affinity is inhibited by 2,3-BPG, and spectrophotometry analysis demonstrated that the injection of 5'-AMP resulted in increased levels of deoxyhemoglobin levels. Consistent with previous studies, our tracing of ^{14}C signal in tissues after injection of radiolabeled 5'-AMP demonstrated highest localization in blood and in vascular tissues such as heart, lung and kidney. Furthermore, *in vitro* treatment of isolated erythrocytes with ^{14}C-AMP showed evidence of direct uptake and metabolism of 5'-AMP. HPLC analysis of the purine products in blood extracts of mice in DH demonstrated that metabolism of 5'-AMP occurs in the blood, and there is a shift in the adenylate equilibrium favoring formation of ADP and decrease in ATP levels. Taken together, these results indicate uptake of 5'-AMP into the erythrocyte is involved in the initiation of the DH state.

Chapter 6

AMP Deaminase in the erythrocyte plays an important role in control of the DH model

AMP deaminase is the major pathway for 5'-AMP catabolism inside the cell.

AMP deaminase catalyzes deamination of 5'-AMP to 5'-inosine monophosphate (5'-IMP), requiring a H_2O molecule and releasing NH_4^+ (14) (Figure 22). IMP can be converted to inosine via cytosolic nucleotidase. Inosine then is converted to hypoxanthine, then xanthine, and then urate. The final product in humans is urate but many species including mice have urate oxidase which creates the final product allantoin (16).

Figure 22: **Adenine nucleotide metabolism pathways inside and outside the cell**
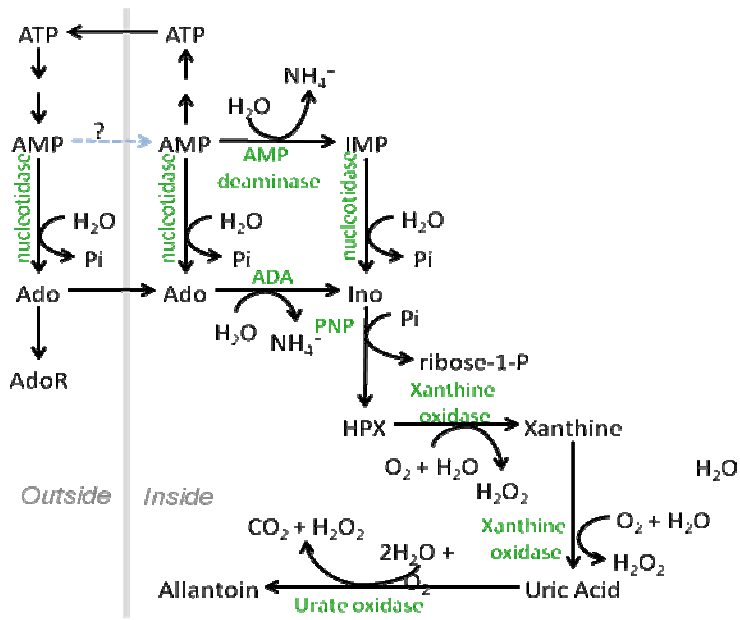
Humans have four isozymes of AMPD that are encoded on different genes. AMPD1, also called myodenylate deaminase, is the main type in skeletal muscle. AMPD2, also called L form, was first isolated from liver, and AMPD3, also called E form, is highly expressed in heart tissue. In humans and other species, many tissues express multiple AMPD isozymes in varying amounts. AMPD3 as well as other AMPD isozymes are expressed in heart and slow-twitch skeletal muscle, but interestingly, erythrocytes only have AMPD3 (46, 47). In humans, AMPD3 has two splice variants: E1 and E2, and the E1 variant is the only type found in erythrocytes. AMPD3 E2 type is found in granulocytes, AMPD2 is found in mononuclear cells, platelets and T-cells, whereas both AMPD3 E1 and AMPD2 are found in B-cells (48-50).

In the literature there are a few described cases of genetic mutation causing a complete lack of AMPD3 in humans. The deficiency was found to be clinically asymptomatic, although there is an increase of steady-state ATP levels to 150% in the affected cells (51). Unlike human AMPD3, murine AMPD3 just has one form; it has no splice variants. It is also called heart AMPD3, because the cDNA was first isolated and cloned from mouse heart, where it is highly expressed (47).

In most mammalian species, erythrocytes lack an enzyme that allows IMP to be converted to 5'-AMP. The conversion of 5'-AMP to IMP is irreversible because the cells lack the enzyme adenylosuccinyl synthetase and thus lack the ability to convert IMP back to AMP (41, 42).

Studying mice deficient in AMPD3 in the erythrocyte could help elucidate the role of AMPD and the erythrocyte in the DH model. Thus, we undertook the generation of mice deficient in AMPD3. Embryonic stem cells with C57Bl/6 background were purchased from Knockout Mouse Project Repository, University of California, Davis, CA. The vector used the "knockout-first" technology to insert the cassette in the intron 1 before the essential exon 2 to create a missense mutation that results in a non-functional mRNA transcript. The cells were injected into the blastocysts of pseudopregnant C57Bl/6 females at the core facility at Institute for Molecular Medicine, Houston, TX, and chimeras were generated. Chimeras were mated with C57Bl/6 mice to generate heterozygous knockouts, and then homozygous knockouts were generated.

AMPD activity is not detectable in erythrocytes and is reduced in heart of AMPD3 deficient mice

To confirm that the gene knockout was successful, it was necessary to measure the AMPD enzyme activity in the tissues of the mice, including the erythrocytes (Figure 23).

Figure 23: AMPD activity is not detectable in the erythrocytes (rbc) and is reduced in the heart of AMPD3 deficient mice. erythrocytes (rbc) n = 15 wild-type and n = 7 AMPD3 deficient. serum n = 10 wild-type and n = 5 AMPD3 deficient. heart n = 8 wild-type and 8 AMPD3 deficient. All other tissues n = 3. Error bars = +/- S.E.M
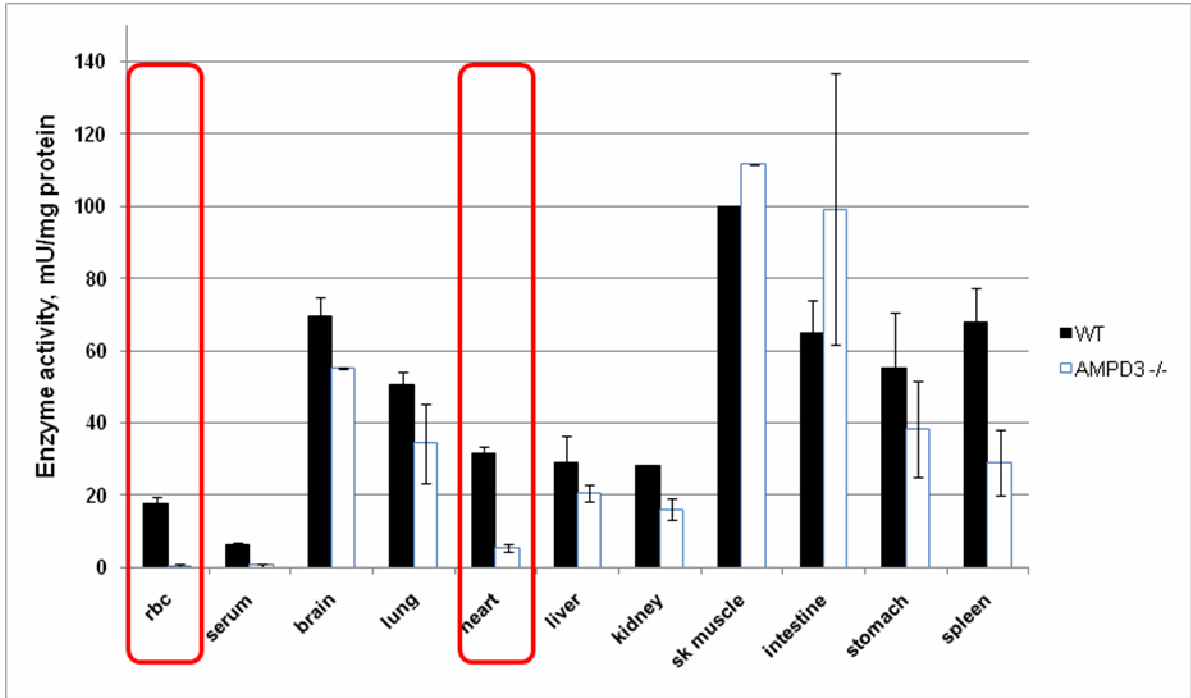
AMPD activity was measured by quantifying the IMP formed in a reaction of tissue lysate using 5'-AMP as previously described (52). In parallel, wild-type mouse tissues were measured as controls. In most tissues, AMPD3 deficient mice had AMPD activity comparable to wild-type. However, there was much lower AMPD activity in heart, as compared to wild-type, and the AMPD activity in the erythrocyte lysate was not detectable. Other isozymes of AMPD are expressed in the heart, so it would be expected to have some AMPD activity. The erythrocyte lysate of heterozygous mice had less AMPD activity than wild-type, but more than the deficient mice (Figure 24). The results demonstrate that the AMPD3 enzyme is not active in the AMPD3 deficient mice.

Figure 24: AMPD activity in erythrocyte lysate of wild-type, heterozygous and homozygous AMPD3 deficient mice. n = 2-3 mice per group, error bars = +/= S.E.M
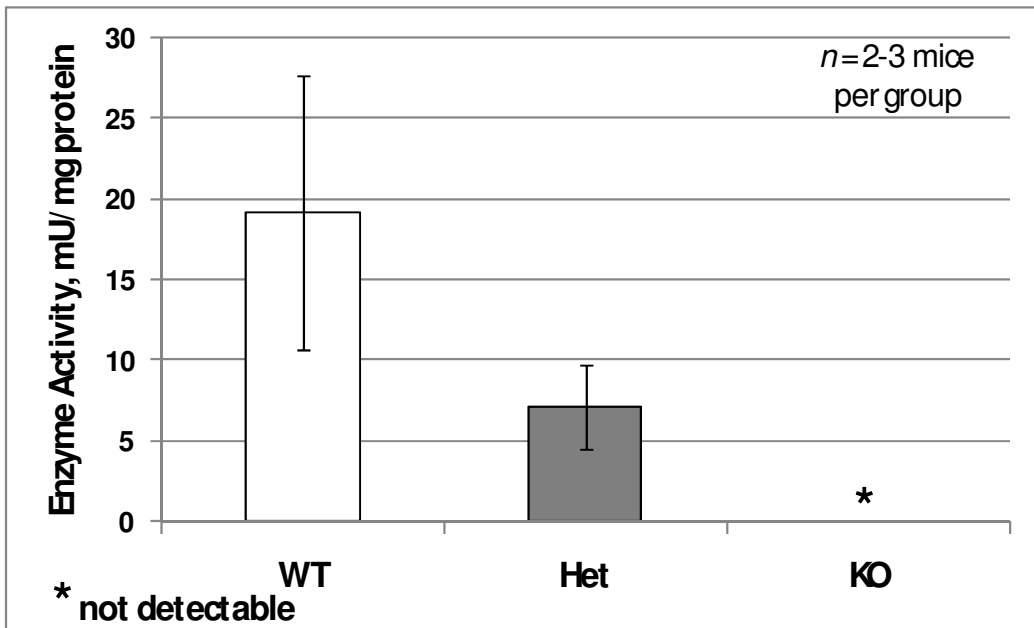
ATP and ADP but not 5'-AMP levels are elevated in the erythrocytes of AMPD3

deficient mice

Next, we investigated whether the loss of AMPD3 will result in elevated

levels of 5'-AMP in the erythrocyte of AMPD3 deficient mice. HPLC analysis was

performed to quantify the levels of ATP, ADP and 5'-AMP in methanol extracts of

erythrocyte lysate (Figure 25).

Figure 25: Erythrocyte lysates of AMPD3 deficient mice have 3-fold higher ATP and ADP levels and similar AMP levels to wild-type mice. Nucleotides from methanol extracts of erythrocyte lysates were separated on HPLC and quantified by calibration curves of standards. *n* = 4, error bars = +/- S.E.M. Student t-test p values: ATP, p = 0.02. ADP, p = 0.04.
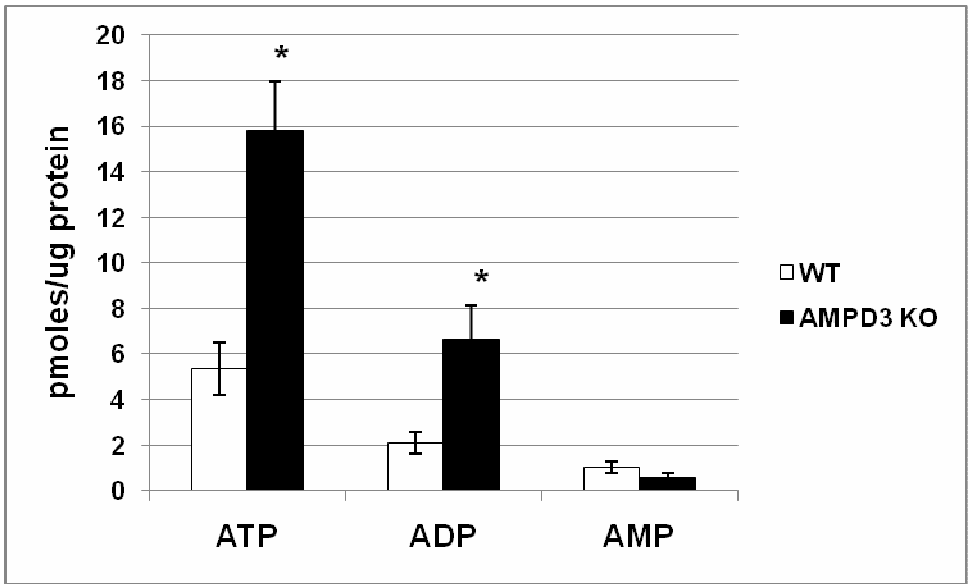
Adenine nucleotide amounts were quantified against calibration curves for ATP, ADP and 5'-AMP, and normalized to the protein concentration in each lysate sample. While the AMP levels were similar to wild-type, AMPD3 deficient erythrocytes had a 3-fold increase in both ATP and ADP levels. These results are contrary to our prediction but are consistent with observation in humans deficient in AMPD3. The affected cells in humans with AMPD3 deficiency have 150% of normal ATP levels, although ADP and 5'-AMP levels are not mentioned (53). A possible explanation for the observation is that the loss of AMPD3 blocks the breakdown of 5'-AMP to IMP. The only catabolic exit for 5'-AMP is via adenosine to inosine by adenosine deaminase (ADA). However, the K_m of ADA is much higher than that of adenosine kinase, which converts adenosine to AMP. Consequently, the adenine nucleotide pool is much larger, and to balance the adenylate equilibrium, both ATP and ADP have to rise, consequently 5'-AMP levels remain low.

AMPD3 deficient mice have similar metabolic rate and glucose utilization to wild-type mice

We then investigated whether the change in the adenylate levels in the erythrocyte will affect metabolic rate of the animals. The calculation for VO_2, mg/kg/h, involves the weight of the animal. We have consistently observed that a lower weight animal tends to have a higher metabolic rate. To overcome this possible artifact, we chose similar weight mice to compare VO_2 between animals. Wild-type, heterozygous and homozygous AMPD3 deficient male mice of similar weight were measured in the CLAMS metabolic chamber for 7 days with free access to food and water, and under 22°C T_a. Our analysis revealed that there was

110

no significant difference in VO_2 for the different genotypes. Average VO_2 of wild-types was 3530 ml/kg/hr, heterozygous mice was 3412 ml/kg/hr and homozygous mice was 3473 ml/kg/hr (Figure 26).

Figure 26: Metabolic rates (VO_2) are similar in similar weight male wild-type, heterozygous and homozygous AMPD3 deficient mice. wild-type $n = 5$, heterozygous $n = 4$, homozygous $n = 7$. Error bars = +/- S.E.M.
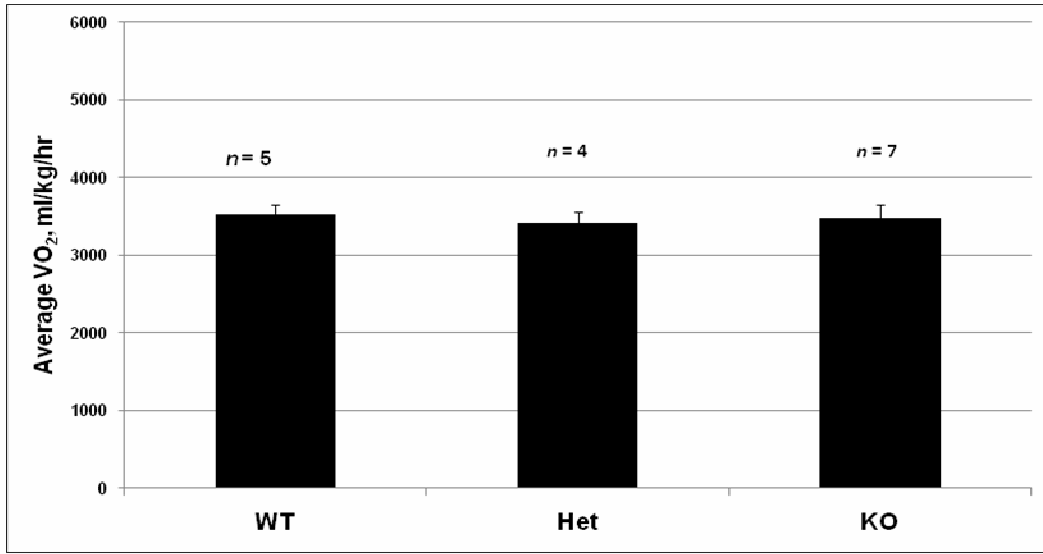
It is well known that ATP/AMP ratio acts as allosteric regulator for key enzymes of glycolysis. Elevated AMP levels signal a need for ATP production, and activate phosphofructokinase 1, a key enzyme in the glycolytic pathway (16). Potentially the change in adenine nucleotide ratio could affect glycolytic rate and therefore blood glucose levels. Thus, we undertook to measure fasting blood glucose in wild-type and AMPD3 deficient mice (Figure 27).

Figure 27: AMPD3 deficient mice have similar fasting blood glucose to wild-type and heterozygous mice. wild-type *n* = 14, heterozygous *n* = 9, homozygous *n* = 16. Error bars = +/- S.E.M.
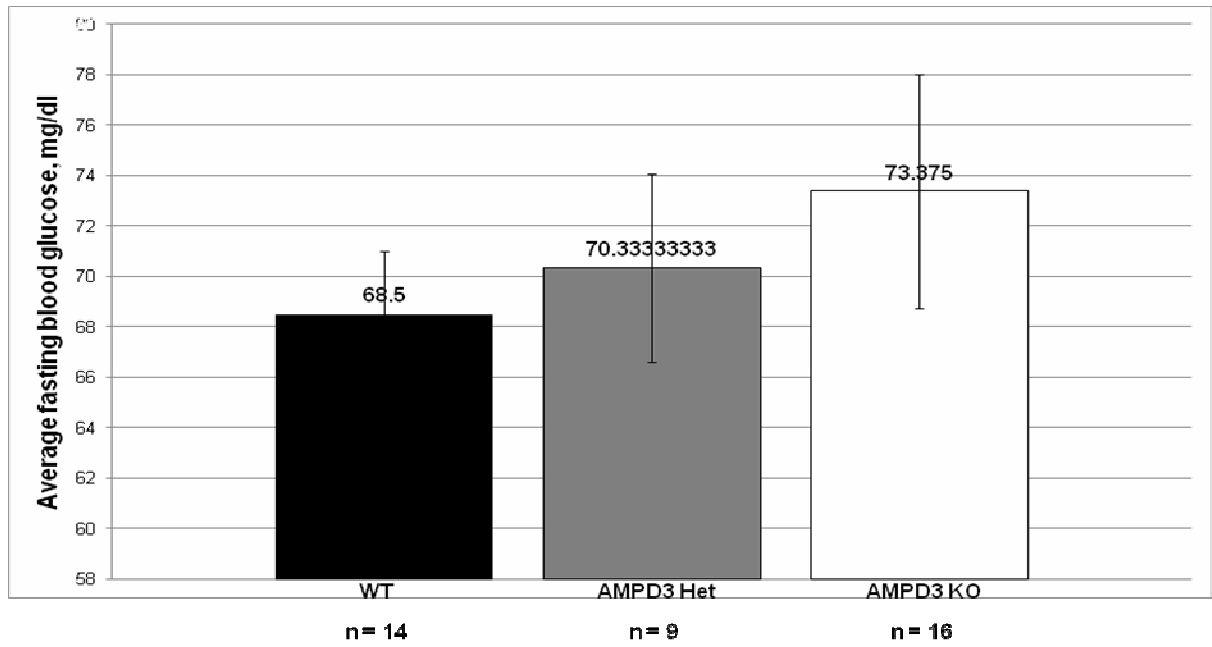
Animals were fasted overnight for 12 hours and then blood glucose was measured the next morning. In a parallel experiment animals were fasted for 12 hours during the day and blood glucose was measured at night. In both experiments, the AMPD3 deficient mice had slightly higher glucose levels, but it was not statistically significant and is within the normal range of fasting blood glucose. The average fasting blood glucose of the wild-type mice was 69 mg/dl, heterozygous mice was 70 mg/dl, and homozygous mice was 73 mg/dl. These studies indicate that glucose utilization was within normal range in AMPD3 deficient mice.

AMPD3 deficient mice have more dramatic response to injection of 5'-AMP

Next we investigated how AMPD3 deficient mice would respond to injection of exogenous 5'-AMP. We predicted that 5'-AMP would be catabolized more slowly in the erythrocytes lacking AMPD3 and they would be more sensitive to 5'-AMP - induced DH. Wild-type and AMPD3 deficient mice were injected with a dose of 5'-AMP and then placed in a 15°C metabolic chamber with free access to food and water. They were monitored and VO_2 was recorded until all the animals recovered from DH. First, a series of dose titration experiments were performed to determine the minimum 5'-AMP dose at which wild-type and AMPD3 deficient mice responded differently. That dose was 0.15 mg/gw 5'-AMP when using 15°C T_a. All the animals experienced the immediate Phase I response after the 5'-AMP injection. The data was analyzed based on length of time in the Phase II response. Since T_b decreases when the VO_2 drops below 1500 ml/kg/h, the average time in Phase II state was

117

used to determine the Phase II response. On average, the AMPD3 deficient mice

stayed in the Phase II response much longer than the wild-type mice (Figure 28).

Figure 28: Male and female AMPD3 deficient mice stay in Phase II response much longer than wild-type mice when injected with a lower dose of 5'-AMP (0.15 mg/gw) and maintained in 15°C T_a. Time in Phase II response is represented as minutes the VO_2 is below 1500 ml/kg/h. females $n = 12$ each group, males $n = 3$. Error bars = +/- S.E.M.

Females
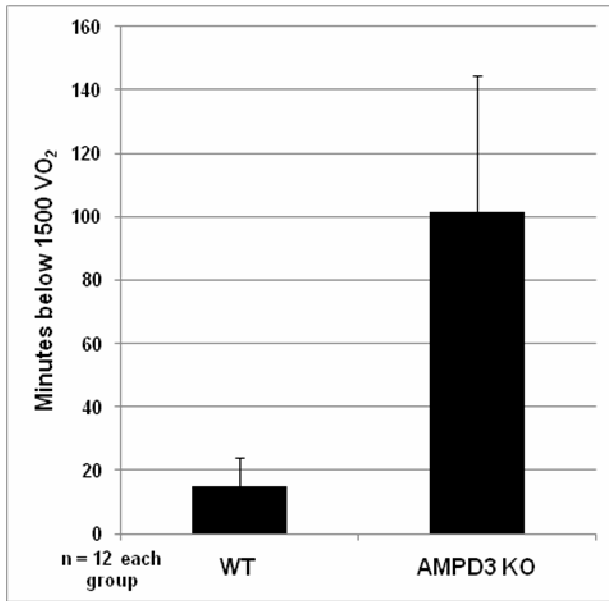
Males
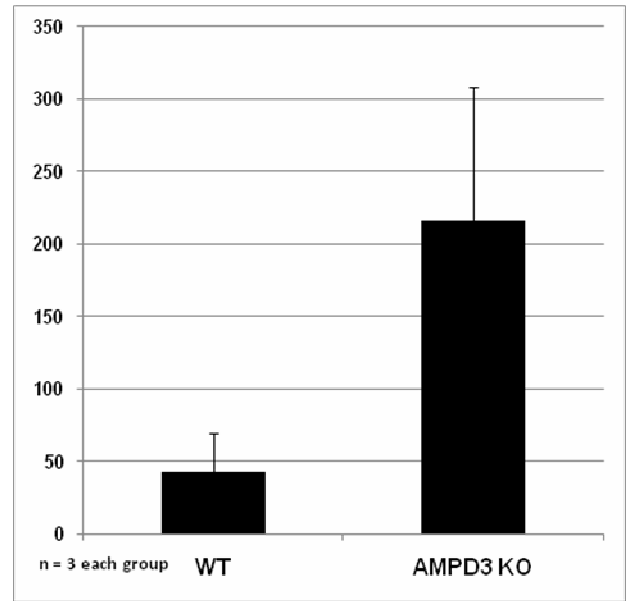
The AMPD3 deficient females stayed in Phase II 81 minutes, compared to wild-type females with an average of 21 minutes. Similarly the AMPD3 deficient males stayed in Phase II for 216 minutes, compared to wild-type male mice which stayed in Phase II for 42 minutes. Thus, the AMPD3 deficient mice stay in Phase II much longer than the wild-type animals, indicating that they were more sensitive to a lower dose of 5'-AMP.

AMPD3 deficient mice have lower core body temperature than wild-type mice

Next, we examined whether the core body temperature of wild-type and AMPD3 deficient mice was normal. Since physical activity or stress can directly impact T_b, we decided to use the telemetry approach for this measurement. Telemetry-chip implanted animals were placed in a 22°C metabolic chamber with free access to food and water, and core body temperature was measured over a period of 7 days (Figure 29).

Figure 29: AMPD3 deficient mice have lower T_b than wild-type mice. T_b of telemetry-implanted mice was measured for 7 days in a 22°C T_a. Error bars = +/- S.E.M., *n*= 7 each group.
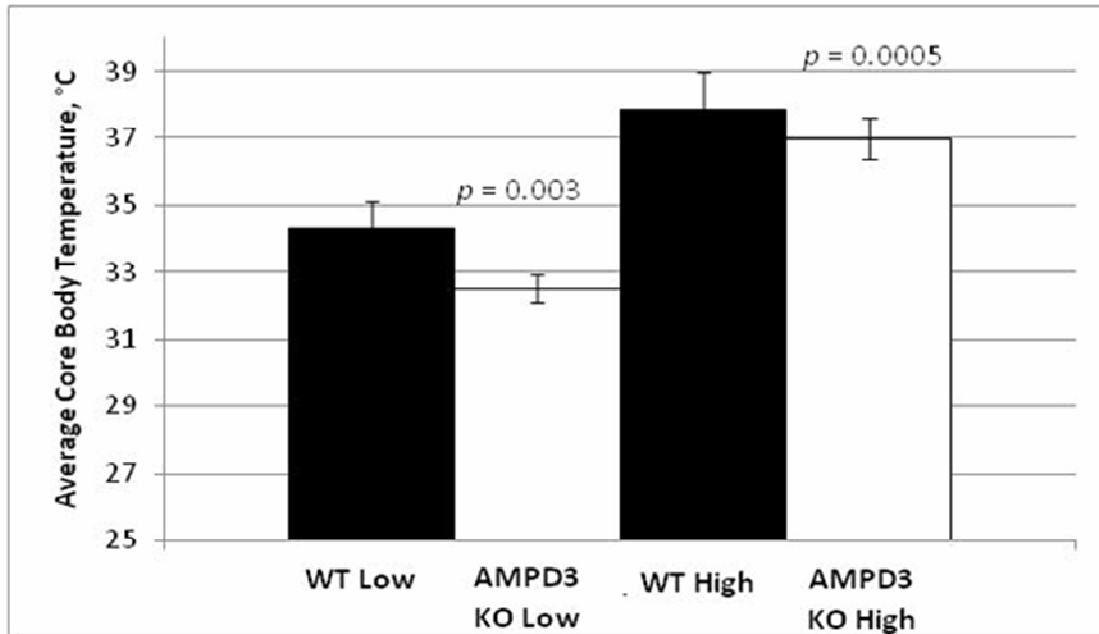
n = 7 each group

To analyze the data, the average of the highest and lowest ten percent recordings was calculated. The average top ten percent readings for the AMPD3 deficient mice was 37.0℃, almost a full degree lower than the wild type mice average of 37.8℃. The average bottom ten percent readings for the AMPD3 deficient mice was 32.5℃, almost 2 degrees lower than the wild type mice average of 34.3℃. It is evident from the graph of the T_b of the wild-type and AMPD3 deficient mice that both genotypes have the normal fluctuations in body temperature throughout the day that correspond to rest and activity. However, in the AMPD3 deficient mice the high and low body temperatures are shifted lower in comparison to wild-type.

AMPD3 deficient mice have difficulty maintaining normal body temperature under moderate metabolic stress

To further explore the AMPD3 deficient mouse phenotype of lower core body temperature, it was important to determine how the animals would react to metabolic stress such as a slight decrease in ambient temperature. Wild-type and AMPD3 deficient mice were placed in the metabolic chamber at 22℃, with free access to food and water for 5 days. Then the ambient temperature in the chamber was decreased to 18℃, and the animals were monitored for two more days. Both groups of mice showed an increase in VO_2 when the ambient temperature decreased. The wild-type mice maintained their T_b, that accompanied the increase in VO_2. However, some AMPD3 deficient mice had a decline in T_b after the ambient temperature decreased, even though their VO_2 had increased (Figure 30). Also, in a few of the mice, it was observed that some AMPD3 deficient mice would

spontaneously enter daily torpor even during the 22°C period (Figure 31). These

observations indicate the AMPD3 deficient mice are impaired in their ability to

maintain core body temperature. It is important to note that under extreme

metabolic stress such as fasting or T_a of 15°C or lower, both wild-type and AMPD3

deficient mice will undergo torpor.

Figure 30: Some AMPD3 deficient mice have reduced ability to maintain T_b when T_a is reduced from 22°C to 18°C, despite increase in VO_2. Representative plot of VO_2 and T_b from one wild-type and one AMPD3 deficient mouse. Note that random outliers in T_b measurement are caused by the positioning of the mouse and telemetry chip to the sensor.

Wild-Type

AMPD3 KO
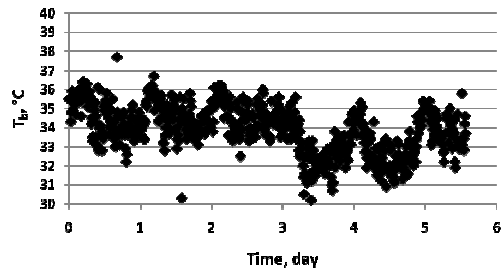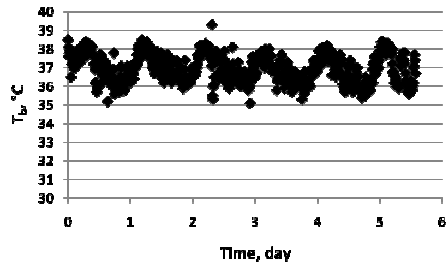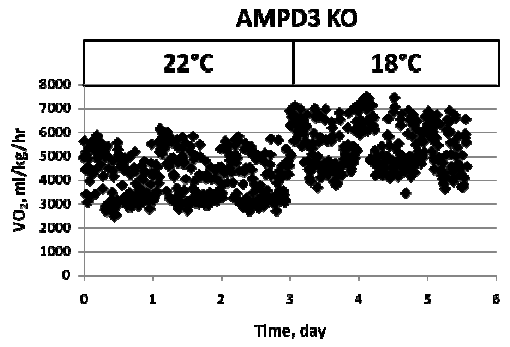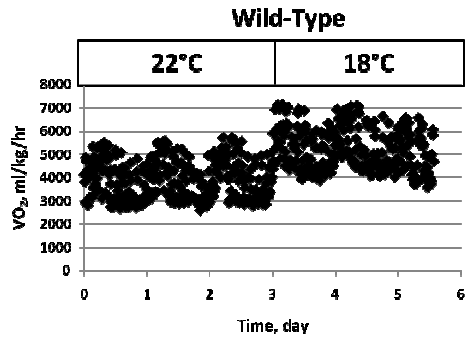
Figure 31: Daily torpor of AMPD3 deficient mice at 22 °C T_a. Representative plot of VO_2 and T_b of an AMPD3 deficent mouse entering torpor in 22 °C and 18 °C T_a, over a period of 6 days with free access to food and water. Note that random outliers in T_b measurement are caused by the positioning of the mouse and telemetry chip to the sensor.

AMPD3 KO
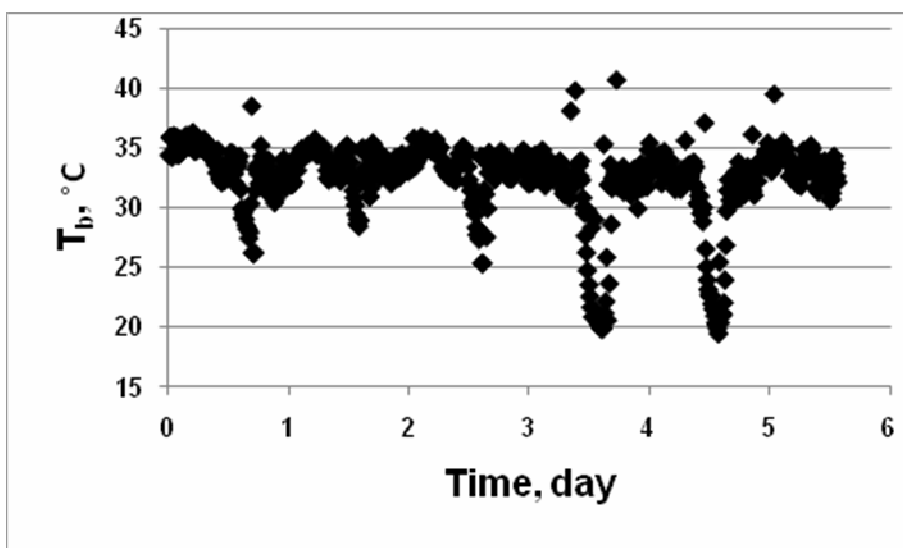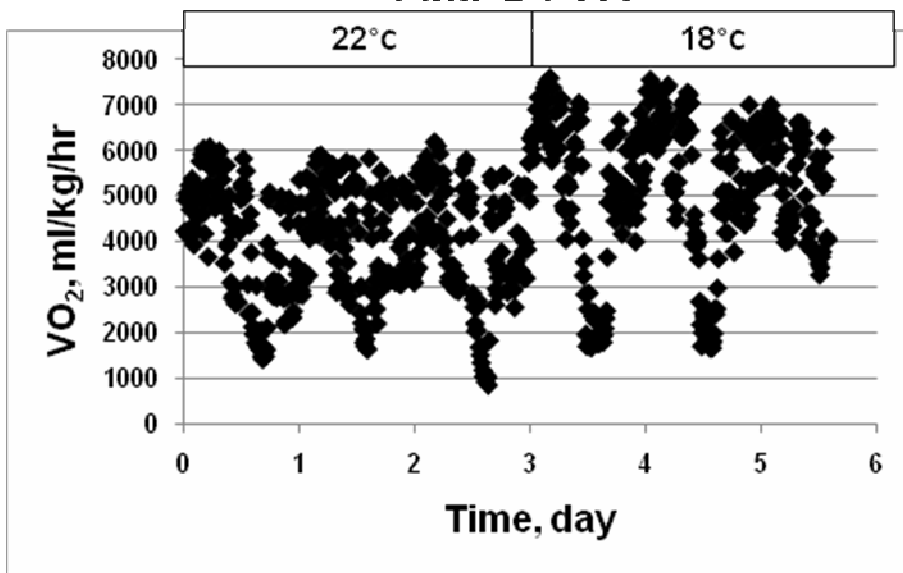
Summary of Results

In summary, AMPD3 deficient mice have similar VO_2 and glucose utilization to wild-type mice. They display a more dramatic response to lower dose 5'-AMP injection than wild-type mice, suggesting that AMPD3 activity, specifically in the erythrocyte, is important to the control of the 5'-AMP – induced model of DH. The increased ATP and ADP in the erythrocytes, their lower T_b phenotype, and the difficulty some of the mice have maintaining T_b during moderate metabolic stress suggest altered energy homeostasis that must be further investigated.

Chapter 7

Discussion and Future Directions

Expression level of most genes in mouse liver are unaltered during DH

The physiological effects of the 5'-AMP injection occur so rapidly (immediately) that the laboratory's initial studies on the mechanism focused on biochemical changes rather than gene expression. However, it was important to determine what changes in gene expression occur after 5'-AMP treatment. A microarray study compared the expression of genes in the liver, a highly metabolic organ, of mice in DH, at arousal, and recovered from DH, compared to control untreated mice. More than 99% of gene expression in the liver was unchanged in DH, compared to untreated animals. In contrast, the arousal stage had much more change in gene expression, with about 200 genes differentially expressed compared to only about 40 genes in the DH state. These results showed that patterns of gene expression are mostly held constant during DH. The expression of circadian genes is stalled as well. Analysis of expression 24 and 48 hours post recovery indicated that the circadian clock takes approximately 24 hours to reset after DH. The cold T_b likely causes the stalling of most gene expression changes in DH (54).

Model for initiation of 5'-AMP - induced deep hypometabolism

Adenosine receptor signaling is known to be involved in thermoregulation and heart rate, both of which undergo dramatic changes in the DH model (37). Since 5'-AMP can be dephosphorylated to adenosine, the initial focus on determining the fate of the injected 5'-AMP was to assess the role of adenosine in initiating DH. Experiments with mice lacking the enzyme 5'-ectonucleotidase/CD73

or the adenosine receptors demonstrated the animals were able to enter DH similarly to wild-type mice. Results from these independent genetic approaches indicated that the dephosphorylation of 5'-AMP to adenosine outside the cell is not required to initiate the DH model.

Next, the focus turned to identifying whether 5'-AMP was the molecule that initiates DH. Experiments showed that mice injected with 5'-CMP and 5'-GMP did not experience a decline in metabolic rate. It was found that adenosine, ATP and ADP do induce a decline in VO_2 but it is more transitory and had slower kinetics than in mice given 5'-AMP. This can be explained because the adenine nucleotides are being modified into 5'-AMP *in vivo*. In contrast adenosine had similar kinetics to 5'-AMP but the effect on VO_2 is very transient. In addition, adenosine has low solubility in water and it has a very short half-life of less than 10 seconds in serum. (36). These factors likely account for the reason mice injected with adenosine did not enter DH, as it is rapidly degraded before DH could take hold. It is possible that given a continuous transfusion, adenosine could induce DH. In comparison with mice injected with 5'-AMP, the VO_2 declined less rapidly in mice given cAMP, and ATP. Other investigators have observed similar results with ADP and ATP given at similar concentration. Together, these results indicate that 5'-AMP itself is responsible for initiating the DH state.

Analysis of ^{14}C signal in perfused tissues after injection of ^{14}C-AMP in a mouse confirmed what had already been found in published data (39). The radiolabel is most concentrated in the blood and in vascular organs such as heart, lung and kidney, and does not concentrate in the brain. In addition, the Mathews

group had found that 5'-[^{11}C]-AMP uptake in blood changed the ADP/ATP ratio, which would occur by the adenylate equilibrium, AMP + ATP $\leftrightarrow$ 2ADP (39). *In vitro* ^{14}C-AMP uptake experiments in erythrocytes isolated from wild-type and CD73 deficient mice and visualized with thin layer chromatography showed that 5'-AMP is taken up in the cells and metabolism favors formation of ADP, which corresponds to the adenylate equilibrium. This information, along with HPLC analysis of blood extracts from mice given 5'-AMP indicated that the 5'-AMP is taken up in the erythrocytes and forces the adenylate equilibrium to increase ADP production, thus reducing ATP levels. Evidence from the metabolomics study and other metabolic analysis of mice treated with 5'-AMP suggested that glycolysis is slowed in mice in DH. Glucose is elevated and lactate is decreased. These data taken together led to the hypothesized model for the initiation step of the DH model (Figure 32).

Figure 32: Proposed model for initiation of 5'-AMP – induced deep hypometabolism
This research was originally published in The Journal of Biological Chemistry.
Daniels IS, Zhang J, O'Brien WG, Tao Z, Miki T, Zhao Z, Blackburn MR, Lee CC.
Title. J Biol Chem. 2010; 285:20716-20723. © the American Society for
Biochemistry and Molecular Biology.

↑Glucose

↑AMP ⤴ ⤻ATP ⇩ HK
↑ADP ⤸ ⤴ ADP⤹

Glucose-6-phosphate

Fructose-6-phosphate

AMP ⤴ ⤻ATP PFK
ADP ⤸ ⤴ ADP⤹

Fructose-1,6-bisphosphate

Dihydroxyacetone phosphate

Glyceraldehyde-3-phosphate

BOGS   1,3-Bisphosphoglycerate

↑2,3-Bisphosphoglycerate   ⤴ADP
                    BOGP   ⤹ATP
                Pi ⤸ ⤻
Hb + O₂ ⇌ HbO₂   3-Phosphoglycerate

2-Phosphoglycerate

Phosphoenolpyruvate
                ⤴ADP
                ⤹ATP
Pyruvate
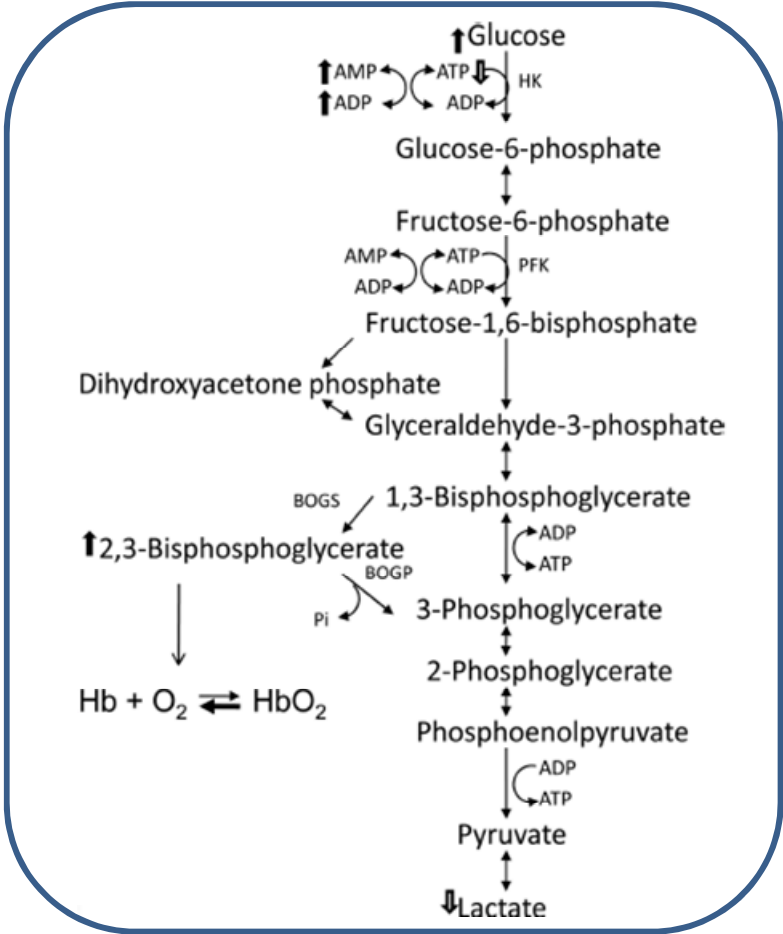
⇩Lactate

The first step of the glycolytic pathway requires ATP for conversion of glucose to glucose-6-phosphate, catalyzed by hexokinase (14). If intracellular ATP levels decrease, then glycolysis would slow and glucose would build up and less lactate, the end product, would be formed. Previous investigators have performed metabolic modeling that indicates when glycolysis slows an increase in 2,3-BPG production occurs in order to stabilize the ATP levels in erythrocytes. Therefore, a small variation in the intracellular ATP level could cause a great increase in 2,3-BPG production in the erythrocyte (40).

2,3-BPG is known to allosterically regulate hemoglobin's affinity for oxygen (16). It binds strongly to deoxyhemoglobin, but binds weakly to oxyhemoglobin (14, 40). Therefore, increased 2,3-BPG in the erythrocytes of an animal injected with 5'-AMP would cause less oxygen transport to tissues. Evidence of this is seen in the physiological observations and measurements of animals injected with 5'-AMP. The Phase I response, in which VO_2 rapidly and dramatically decreases, may be a reflection of the sudden reduction in oxygen transport to tissues. Also, the allosteric nature of 2,3-BPG regulation of hemoglobin affinity for oxygen could be the reason that a range of doses of 5'-AMP all trigger a Phase I response of similar magnitude. The elevated 2,3-BPG levels are further confirmed by the spectral analysis of blood taken 10 minutes after 5'-AMP injection showing increased deoxyhemoglobin and decreased oxyhemoglobin levels. The reduced oxygen transport to the tissues could trigger a whole body physiological response to lower metabolic rate. If this occurs in a cooler environment, then the body will lose heat and be unable to maintain euthermic T_b due to the lower metabolic rate. T_b will continue to decrease

toward the T_a. During the Phase II response, in which T_b gradually decreases as VO_2 continues to decline, the body would not require as much oxygen, which in turn allows the VO_2 to drop further. As demonstrated by experiments measuring time to recovery from DH in different T_a, the correct T_a will allow the animal to maintain the DH state, and the animal's T_b and the T_a will be in equilibrium. If the animal in DH is gradually rewarmed, the VO_2 will increase, causing arousal from DH. However, there is much variation in the how long mice maintained in the same T_a remain in DH, which suggests there are still factors to be determined that control the length of time in DH.

Discussion of erythrocyte as initiation site for 5'-AMP – induced deep hypometabolism

Metabolic rate in small mammals can be pharmacologically reduced by treatment with 2-deoxyglucose or hydrogen sulfide gas (H_2S) (22, 55). While it is not understood how these metabolic inhibitors reduce T_b, the effects on erythrocytes are known. Erythrocytes metabolize inhaled H_2S gas in the following reaction: HbO_2 + H_2S → $2S$ + Hb + H_2O, and oxygen levels are greatly decreased (23). In the case of 2-deoxyglucose, a known inhibitor of hexokinase, the first step in glycolysis is stopped. Since erythrocytes rely primarily on glycolysis to produce ATP, the cellular level of ATP would decrease. The role of the erythrocyte in 2-deoxyglucose induction of torpor is further suggested because a different metabolic inhibitor, β-mercaptoacetate, does not induce torpor in small mammals. β-mercaptoacetate inhibits β-oxidation, a function of mitochondria. Erythrocytes lack mitochondria (14, 55). Further evidence of the role of the erythrocyte is that previous investigators

have used exsanguination to reduce T_b in mammals (56, 57). Also, hypoxia is known to cause hypothermia (58). In summary, the results suggest the erythrocyte may be the site for the initiation of many different methods of reducing metabolic rate in mammals.

Discussion of AMPD3 deficient mice phenotype and AMPD3 role in 5'-AMP-induced model of deep hypometabolism

The determination that the erythrocyte is the site of initiation of the DH model led to studies to determine whether AMP deaminase, specifically in the erythrocyte, plays a role in the control of the DH model. AMPD3 deficient mice had undetectable AMPD activity in erythrocytes, and reduced activity in heart tissue as evident from the lack of IMP formation in the erythrocyte lysates.

AMPD3 deficient mice remaining in Phase II response longer than wild-type mice after lower dosage of 5'-AMP indicates that the AMPD catabolism of 5'-AMP, specifically in the erythrocyte, is important in the 5'-AMP – induced DH model. Future investigations will test whether AMPD3/CD73 deficient mice injected with lower dose 5'- AMP have an even more dramatic response than the AMPD3 deficient mice. Lack of 5'-AMP catabolism outside the cell by CD73, combined with a lack of 5'-AMP catabolism inside the cell by AMPD3 could possibly cause a low 5'-AMP dose to be effectively higher in these mice.

We observed that the VO_2 was similar in wild-type, heterozygous and homozygous AMPD3 deficient mice. A similar glucose level in fasting blood glucose experiments also suggested the AMPD3 deficient mice have similar metabolic

phenotype to wild-type, at least under normal metabolic state. However, analysis of the T_b of telemetry implanted AMPD3 deficient mice showed a lower T_b in constant 22°C T_a, and some have difficulty maintaining T_b under moderate metabolic stress.

Observation of the lower T_b phenotype led to the question of how the T_b could be reduced without such apparent decrease in metabolic rate. Classically, T_b regulation is controlled by the hypothalamus. The AMPD3 deficient mice are lacking the AMPD activity only in the erythrocyte, so the hypothalamic thermoregulation may not be directly affected by this genetic mutation. Rather, we speculate that when under metabolic stress, delivery of oxygen to the tissue is important for maintaining T_b. If the function of the erythrocyte is somehow impaired, the delivery of oxygen to tissues may be inadequate. Hypoxia is known to decrease thermogenesis (59). Investigators have found that brown adipose tissue of rats maintained in hypoxic conditions since birth had greatly reduced uncoupling protein content (59). Also, studies in CD-1 mice demonstrated that chronic hypoxia reduces capacity for non-shivering thermogenesis and decreases the relative contents of uncoupling protein 1 in brown adipose tissue and uncoupling protein 3 in gastrocnemius muscle (15). Interestingly, chronically hypoxic CD-1 mice had a decline in T_b to 35°C when placed in a 4°C T_a, although their VO_2 increased similarly to that of normoxic control mice. In contrast, the normoxic control mice maintained euthermic T_b of 37°C in this acute metabolic stress condition (15). These findings correspond to our observations in AMPD3 deficient mice. When T_a was reduced from 22°C to 18°C, some AMPD3 deficient mice displayed inability to maintain T_b despite a similar increase in VO_2 to wild-type mice. Further studies will investigate

the possibility that AMPD3 deficiency in mice impairs erythrocyte function, causing mild chronic hypoxia, and consequently undermining non-shivering thermogenesis capacity. Analysis of the brown adipose tissue and muscle uncoupling protein content, and oxygenation status in the erythrocyte and tissues will give insight into this question.

Possible explanations for increased ATP and ADP in erythrocytes of AMPD3 deficient mice

Analysis of the ATP, ADP and 5'-AMP levels in the erythrocyte lysate extracts of the AMPD3 deficient mice showed that ATP and ADP are increased 3-fold. This corresponds with published data describing 150% of normal level of ATP in affected cells of humans with AMPD3 deficiency (51). In addition, analysis of aged erythrocytes from rabbits demonstrate that erythrocyte AMP deaminase activity reaches a minimum after 40 days in the 120 day erythrocyte lifespan. The aged erythrocytes have elevated levels of ATP (60).

It has not been explained in the literature how ATP levels can rise when erythrocytes lack AMPD3 to deaminate 5'-AMP to IMP. Cytosolic nucleotidase dephosphorylates 5'-AMP to adenosine, but adenosine kinase which phosphorylates adenosine back to 5'-AMP has a much lower K_m than adenosine deaminase, so phosphorylation of adenosine to 5'-AMP is favored. Thus, if catabolism of 5'-AMP to IMP is blocked, then the adenine nucleotide pool would be increased. By the adenylate equilibrium AMP + ATP $\leftrightarrow$ 2 ADP, if 5'-AMP levels rise, then to balance the equilibrium, ADP would have to increase and ATP should

decrease. Alternatively, the rise in ADP could be balanced by a rise in ATP and a decline in 5'-AMP, which is what was observed.

Cytosolic nucleotidase can dephosphorylate AMP to adenosine, but then in the next step adenosine kinase has a much lower K_m than adenosine deaminase, so phosphorylation of adenosine to AMP is favored (Figure 33) (14, 16, 60).

Figure 33: K_m values for metabolism of adenine nucleotides and nucleosides inside the cell
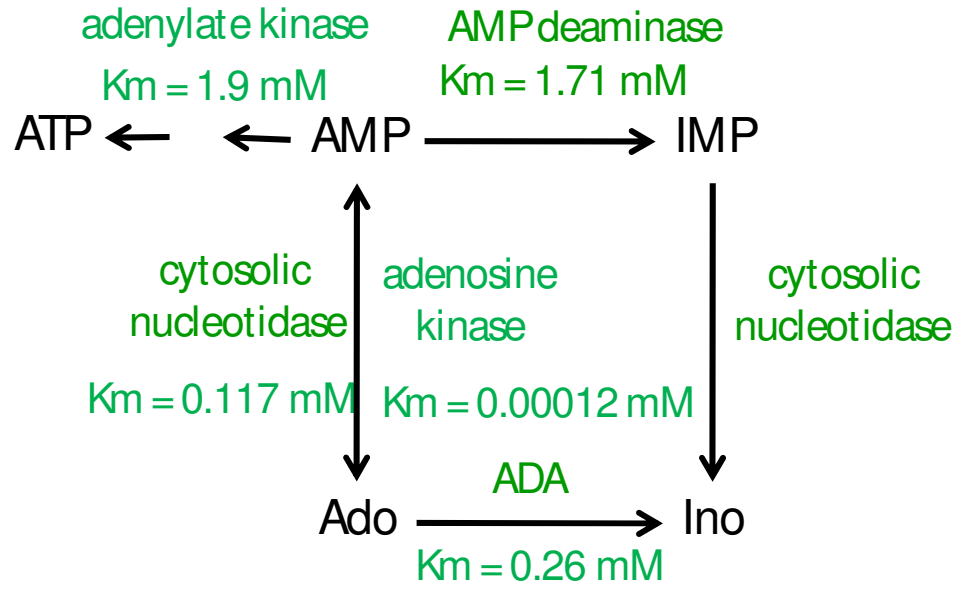
AMP formation would be favored until the substrate level was high enough to overcome the lower K_m of adenosine kinase, and allow adenosine deaminase to convert some of the adenosine to inosine. This would cause a build-up of AMP, which can be phosphorylated to ADP and ATP.

Possible role of Na$^+$/K$^+$ pump

Physiological concentration of 5'-AMP is much lower than ATP and ADP. In erythrocytes, 5'-AMP concentration is about 14 µM, compared to 1,797 µM for ATP and 227 µM for ADP (61). Maintaining the relative concentrations of ATP, ADP and 5'-AMP inside the cell is essential.

One possible reason for the adenine nucleotide pool in AMPD3 deficient erythrocytes to be maintained in ATP/ADP rather than 5'-AMP/ADP is the physiological need of the erythrocytes. The observed increase in ATP and ADP levels in the erythrocyte lysate are within the normal ADP/ATP ratio. Maintenance of this ratio would promote proper function of the Na$^+$/K$^+$ pump. The Na$^+$/K$^+$ pump, also called the Na$^+$/K$^+$– ATPase, uses active transport to export Na$^+$ and import K$^+$, using the energy from dephosphorylation of ATP to ADP (62). One of its functions is to maintain the osmotic pressure within the cell, which is necessary to maintain cell shape. Previous studies have investigated the effect of changing the ADP/ATP ratio on the activity of the Na$^+$/K$^+$ pump in resealed erythrocyte ghosts. The investigators used phosphoarginine or phosphocreatine-based systems to enzymatically regenerate ADP or ATP to vary ADP/ATP ratios. Using an adenylate kinase inhibitor, they prevented the adenylate equilibrium from re-equilibrating the AMP,

ADP and ATP to normal ratios. Changes in ADP/ATP ratio affected the rate of ion exchange (63). This could have significant impact on the homeostasis of intact erythrocytes.

The energy homeostasis in erythrocytes of AMPD3 deficient mice may be altered due to increased adenine nucleotide pools. This could cause an inability of the erythrocytes to properly transport oxygen to tissues, which may result in the decreased T_b phenotype. Further analysis is needed to understand this phenotype.

Conclusion

In summary, this dissertation describes a novel method for inducing a deep hypometabolic state in mammals, induced by uptake and metabolism of a natural molecule, 5'-AMP. Biochemical analyses and genetic approaches have provided clues into the initiation and control of the model. This work adds to understanding of the mechanisms involved in the 5'-AMP induced model of deep hypometabolism. Possible future clinical application of the model in humans will require a deeper comprehension of the mechanisms underlying this model.

Bibliography

1.   Heldmaier, G., Ortmann, S., and Elvert, R. 2004. Natural hypometabolism during hibernation and daily torpor in mammals. *Respir Physiol Neurobiol* 141:317-329.

2.   Song, X., Kortner, G., and Geiser, F. 1995. Reduction of metabolic rate and thermoregulation during daily torpor. *J Comp Physiol B* 165:291-297.

3.   Geiser, F. 2010. Aestivation in mammals and birds. *Prog Mol Subcell Biol* 49:95-111.

4.   Dausmann, K.H., Glos, J., Ganzhorn, J.U., and Heldmaier, G. 2005. Hibernation in the tropics: lessons from a primate. *J Comp Physiol B* 175:147-155.

5.   Toien, O., Blake, J., Edgar, D.M., Grahn, D.A., Heller, H.C., and Barnes, B.M. 2011. Hibernation in black bears: independence of metabolic suppression from body temperature. *Science* 331:906-909.

6.   Ruby, N.F., and Zucker, I. 1992. Daily torpor in the absence of the suprachiasmatic nucleus in Siberian hamsters. *Am J Physiol* 263:R353-362.

7.   Kondo, N., and Kondo, J. 1992. Identification of novel blood proteins specific for mammalian hibernation. *J Biol Chem* 267:473-478.

8.   Kondo, N., Sekijima, T., Kondo, J., Takamatsu, N., Tohya, K., and Ohtsu, T. 2006. Circannual control of hibernation by HP complex in the brain. *Cell* 125:161-172.

9.   Revel, F.G., Herwig, A., Garidou, M.L., Dardente, H., Menet, J.S., Masson-
      Pevet, M., Simonneaux, V., Saboureau, M., and Pevet, P. 2007. The
      circadian clock stops ticking during deep hibernation in the European
      hamster. *Proc Natl Acad Sci U S A* 104:13816-13820.

10.   Ruby, N.F., Dark, J., Heller, H.C., and Zucker, I. 1996. Ablation of
      suprachiasmatic nucleus alters timing of hibernation in ground squirrels. *Proc
      Natl Acad Sci U S A* 93:9864-9868.

11.   Heldmaier, G., Klingenspor, M., Werneyer, M., Lampi, B.J., Brooks, S.P., and
      Storey, K.B. 1999. Metabolic adjustments during daily torpor in the
      Djungarian hamster. *Am J Physiol* 276:E896-906.

12.   Martini, F.H. 1998. *Fundamentals of Anatomy and Physiology*. Upper Saddle
      River, NJ: Prentice Hall, Inc.

13.   Conti, B., Sanchez-Alavez, M., Winsky-Sommerer, R., Morale, M.C., Lucero,
      J., Brownell, S., Fabre, V., Huitron-Resendiz, S., Henriksen, S., Zorrilla, E.P.,
      et al. 2006. Transgenic mice with a reduced core body temperature have an
      increased life span. *Science* 314:825-828.

14.   Lehninger, A. 1982. *Principles of Biochemistry*. New York: W. H. Freeman.

15.   Beaudry, J.L., and McClelland, G.B. 2010. Thermogenesis in CD-1 mice after
      combined chronic hypoxia and cold acclimation. *Comp Biochem Physiol B
      Biochem Mol Biol* 157:301-309.

16.   Stryer, L. 1981. *Biochemistry*. San Francisco: W. H. Freeman and Company.

17. Stamper, J.L., Dark, J., and Zucker, I. 1999. Photoperiod modulates torpor and food intake in Siberian hamsters challenged with metabolic inhibitors. *Physiol Behav* 66:113-118.

18. Scanlan, T.S. 2011. Endogenous 3-Iodothyronamine (T1AM): More Than We Bargained For. *J Clin Endocrinol Metab* 96:1674-1676.

19. Scanlan, T.S., Suchland, K.L., Hart, M.E., Chiellini, G., Huang, Y., Kruzich, P.J., Frascarelli, S., Crossley, D.A., Bunzow, J.R., Ronca-Testoni, S., et al. 2004. 3-Iodothyronamine is an endogenous and rapid-acting derivative of thyroid hormone. *Nat Med* 10:638-642.

20. Barros, R.C., Branco, L.G., and Carnio, E.C. 2006. Respiratory and body temperature modulation by adenosine A1 receptors in the anteroventral preoptic region during normoxia and hypoxia. *Respir Physiol Neurobiol* 153:115-125.

21. Blackstone, E., and Roth, M.B. 2007. Suspended animation-like state protects mice from lethal hypoxia. *Shock* 27:370-372.

22. Blackstone, E., Morrison, M., and Roth, M.B. 2005. H2S induces a suspended animation-like state in mice. *Science* 308:518.

23. Evans, C.L. 1967. The toxicity of hydrogen sulphide and other sulphides. *Q J Exp Physiol Cogn Med Sci* 52:231-248.

24. Bailes, J.E., Leavitt, M.L., Teeple, E., Jr., Maroon, J.C., Shih, S.R., Marquardt, M., Rifai, A.E., and Manack, L. 1991. Ultraprofound hypothermia with complete blood substitution in a canine model. *J Neurosurg* 74:781-788.

25. Frerichs, K.U., and Hallenbeck, J.M. 1998. Hibernation in ground squirrels induces state and species-specific tolerance to hypoxia and aglycemia: an in vitro study in hippocampal slices. *J Cereb Blood Flow Metab* 18:168-175.

26. Wang, H., Olivero, W., Wang, D., and Lanzino, G. 2006. Cold as a therapeutic agent. *Acta Neurochir (Wien)* 148:565-570; discussion 569-570.

27. Hammer, M.D., and Krieger, D.W. 2002. Acute ischemic stroke: is there a role for hypothermia? *Cleve Clin J Med* 69:770, 773-774, 776-777 passim.

28. Testa, G., Schaft, J., van der Hoeven, F., Glaser, S., Anastassiadis, K., Zhang, Y., Hermann, T., Stremmel, W., and Stewart, A.F. 2004. A reliable lacZ expression reporter cassette for multipurpose, knockout-first alleles. *Genesis* 38:151-158.

29. Zhang, J., Kaasik, K., Blackburn, M.R., and Lee, C.C. 2006. Constant darkness is a circadian metabolic signal in mammals. *Nature* 439:340-343.

30. Olsen, O., Schaffalitzky de Muckadell, O.B., Cantor, P., Erlanson-Albertsson, C., Hansen, C.P., and Worning, H. 1988. Effect of trypsin on the hormonal regulation of the fat-stimulated human exocrine pancreas. *Scand J Gastroenterol* 23:875-881.

31. Lowe, M.E. 1997. Molecular mechanisms of rat and human pancreatic triglyceride lipases. *J Nutr* 127:549-557.

32. D'Agostino, D., Cordle, R.A., Kullman, J., Erlanson-Albertsson, C., Muglia, L.J., and Lowe, M.E. 2002. Decreased postnatal survival and altered body weight regulation in procolipase-deficient mice. *J Biol Chem* 277:7170-7177.

33. Daniels, I.S., Zhang, J., O'Brien, W.G., 3rd, Tao, Z., Miki, T., Zhao, Z., Blackburn, M.R., and Lee, C.C. 2010. A role of erythrocytes in adenosine monophosphate initiation of hypometabolism in mammals. *J Biol Chem* 285:20716-20723.

34. Swindle, M.M., Makin, A., Herron, A.J., Clubb, F.J., Jr., and Frazier, K.S. 2011. Swine as Models in Biomedical Research and Toxicology Testing. *Vet Pathol*.

35. Swoap, S.J., Rathvon, M., and Gutilla, M. 2007. AMP does not induce torpor. *Am J Physiol Regul Integr Comp Physiol* 293:R468-473.

36. Paul, T., and Pfammatter, J.P. 1997. Adenosine: an effective and safe antiarrhythmic drug in pediatrics. *Pediatr Cardiol* 18:118-126.

37. Yang, J.N., Chen, J.F., and Fredholm, B.B. 2009. Physiological roles of A1 and A2A adenosine receptors in regulating heart rate, body temperature, and locomotion as revealed using knockout mice and caffeine. *Am J Physiol Heart Circ Physiol* 296:H1141-1149.

38. Jacobson, K.A., and Gao, Z.G. 2006. Adenosine receptors as therapeutic targets. *Nat Rev Drug Discov* 5:247-264.

39. Mathews, W.B., Nakamoto, Y., Abraham, E.H., Scheffel, U., Hilton, J., Ravert, H.T., Tatsumi, M., Rauseo, P.A., Traughber, B.J., Salikhova, A.Y., et al. 2005. Synthesis and biodistribution of [11C]adenosine 5'-monophosphate ([11C]AMP). *Mol Imaging Biol* 7:203-208.

40. Mulquiney, P.J., Bubb, W.A., and Kuchel, P.W. 1999. Model of 2,3-bisphosphoglycerate metabolism in the human erythrocyte based on detailed

enzyme kinetic equations: in vivo kinetic characterization of 2,3-bisphosphoglycerate synthase/phosphatase using 13C and 31P NMR. *Biochem J* 342 Pt 3:567-580.

41. Lowy, B.A., Williams, M.K., and London, I.M. 1962. Enzymatic deficiencies of purine nucleotide synthesis in the human erythrocyte. *J Biol Chem* 237:1622-1625.

42. Lowy, B., and Dorfman, B.Z. 1970. Adenylosuccinase activity in human and rabbit erythrocyte lysates. *J Biol Chem* 245:3043-3046.

43. Wu, C.P., Woodcock, H., Hladky, S.B., and Barrand, M.A. 2005. cGMP (guanosine 3',5'-cyclic monophosphate) transport across human erythrocyte membranes. *Biochem Pharmacol* 69:1257-1262.

44. Tsukamoto, T., Suyama, K., Germann, P., and Sonenberg, M. 1980. Adenosine cyclic 3',5'-monophosphate uptake and regulation of membrane protein kinase in intact human erythrocytes. *Biochemistry* 19:918-924.

45. Kolassa, N., and Pfleger, K. 1975. Adenosine uptake by erythrocytes of man, rat and guinea-pig and its inhibition by hexobendine and dipyridamole. *Biochem Pharmacol* 24:154-156.

46. Thakkar, J.K., Janero, D.R., Sharif, H.M., and Yarwood, C. 1995. Mammalian-heart adenylate deaminase: cross-species immunoanalysis of tissue distribution with a cardiac-directed antibody. *Mol Cell Biochem* 145:177-183.

47. Wang, X., Morisaki, H., Sermsuvitayawong, K., Mineo, I., Toyama, K., Ogasawara, N., Mukai, T., and Morisaki, T. 1997. Cloning and expression of cDNA encoding heart-type isoform of AMP deaminase. *Gene* 188:285-290.

48. Ogasawara, N., Goto, H., and Yamada, Y. 1984. AMP deaminase isozymes in human blood cells. *Adv Exp Med Biol* 165 Pt B:59-62.

49. Ogasawara, N., Goto, H., Yamada, Y., Watanabe, T., and Asano, T. 1982. AMP deaminase isozymes in human tissues. *Biochim Biophys Acta* 714:298-306.

50. Mahnke-Zizelman, D.K., and Sabina, R.L. 1992. Cloning of human AMP deaminase isoform E cDNAs. Evidence for a third AMPD gene exhibiting alternatively spliced 5'-exons. *J Biol Chem* 267:20866-20877.

51. Ogasawara, N., Goto, H., Yamada, Y., and Hasegawa, I. 1986. Deficiency of erythrocyte type isozyme of AMP deaminase in human. *Adv Exp Med Biol* 195 Pt A:123-127.

52. Mahnke-Zizelman, D.K., Tullson, P.C., and Sabina, R.L. 1998. Novel aspects of tetramer assembly and N-terminal domain structure and function are revealed by recombinant expression of human AMP deaminase isoforms. *J Biol Chem* 273:35118-35125.

53. Ogasawara, N., Goto, H., Yamada, Y., Nishigaki, I., Itoh, T., Hasegawa, I., and Park, K.S. 1987. Deficiency of AMP deaminase in erythrocytes. *Hum Genet* 75:15-18.

54. Zhao, Z., Miki, T., Van Oort-Jansen, A., Matsumoto, T., Loose, D.S., and Lee, C.C. 2011. Hepatic gene expression profiling of 5'-AMP-induced hypometabolism in mice. *Physiol Genomics* 43:325-345.

55. Dark, J., Miller, D.R., and Zucker, I. 1994. Reduced glucose availability induces torpor in Siberian hamsters. *Am J Physiol* 267:R496-501.

56. Rhee, P., Talon, E., Eifert, S., Anderson, D., Stanton, K., Koustova, E., Ling, G., Burris, D., Kaufmann, C., Mongan, P., et al. 2000. Induced hypothermia during emergency department thoracotomy: an animal model. *J Trauma* 48:439-447; discussion 447-450.

57. Ikeda, S. 1965. Exsanguination cooling. *Tohoku J Exp Med* 87:185-198.

58. Wood, S.C. 1991. Interactions between hypoxia and hypothermia. *Annu Rev Physiol* 53:71-85.

59. Mortola, J.P., and Naso, L. 1997. Brown adipose tissue and its uncoupling protein in chronically hypoxic rats. *Clin Sci (Lond)* 93:349-354.

60. Dale, G.L., and Norenberg, S.L. 1989. Time-dependent loss of adenosine 5'-monophosphate deaminase activity may explain elevated adenosine 5'-triphosphate levels in senescent erythrocytes. *Blood* 74:2157-2160.

61. Rapaport, E., and Fontaine, J. 1989. Anticancer activities of adenine nucleotides in mice are mediated through expansion of erythrocyte ATP pools. *Proc Natl Acad Sci U S A* 86:1662-1666.

62. Boldyrev, A.A. 1993. Functional activity of Na+,K(+)-pump in normal and pathological tissues. *Mol Chem Neuropathol* 19:83-93.

63.   Kennedy, B.G., Lunn, G., and Hoffman, J.F. 1986. Effects of altering the

ATP/ADP ratio on pump-mediated Na/K and Na/Na exchanges in resealed

human red blood cell ghosts. *J Gen Physiol* 87:47-72.

Vita

Isadora Susan Daniels was born in Lawrence, Kansas on September 3, 1974, the daughter of Eugenia J. Daniels and James B. Daniels. After completing her work at M.B. Lamar High School, Houston, Texas in 1992, she entered Texas A&M University in College Station, Texas. She transferred to The University of Texas at Austin in 1993 and completed her Bachelor of Arts degree with a major in Journalism in December, 1996. For several years she worked in academic advising and student development, first at The University of Texas at Austin and then at Lone Star College-Montgomery in Conroe, Texas. She had always had a strong interest in science, so began taking the science and mathematics night courses to enter graduate school while working full time. She worked as a research technician in the Department of Pathology and Laboratory Medicine for one year before entering The University of Texas Health Science Center at Houston Graduate School of Biomedical Sciences in January of 2006. She joined the Biochemistry and Molecular Biology Program and will graduate with her Doctorate of Philosophy in August 2011.

Permanent address:
1316 Dennis St.
Houston, TX 77006